



Climate change impacts on the leaching of a heavy metal contamination in a small lowland catchment

Ate Visser ^{a,b,*}, Joop Kroes ^c, Michelle T.H. van Vliet ^c, Stephen Blenkinsop ^d, Hayley J. Fowler ^d, Hans Peter Broers ^{a,e,f}

^a Deltares, Princetonlaan 6, P.O. Box 85467, 3508 AL Utrecht, The Netherlands

^b Lawrence Livermore National Laboratory, 7000 East Avenue, Livermore, CA 94550-9234, USA

^c Wageningen University and Research Centre, Droevendaalsesteeg 4, P.O. Box 47, 6700 AA Wageningen, The Netherlands

^d Water Resource Systems Research Laboratory, School of Civil Engineering and Geosciences, Cassie Building, Newcastle University, Newcastle Upon Tyne NE1 7RU, England, UK

^e TNO Geological Survey of the Netherlands, P.O. Box 80015, 3584 TA, Utrecht, The Netherlands

^f VU University Amsterdam, Department of Hydrology and Geo-Environmental Sciences, De Boelelaan 1085-1087, 1081 HV Amsterdam, The Netherlands

ARTICLE INFO

Article history:

Received 15 October 2010

Received in revised form 15 April 2011

Accepted 28 April 2011

Available online 7 May 2011

Keywords:

Climate change

Surface water quality

Heavy metal contamination

Downscaling

ABSTRACT

The Keersop catchment (43 km²) in the south of The Netherlands has been contaminated by the emissions of four zinc ore smelters. The objective of this study was to assess the effects of future projected climate change on the hydrology and the leaching of heavy metals (i.e. Cd and Zn) in the catchment. The numerical, quasi-2D, unsaturated zone Soil Water Atmosphere Plant model was used with 100-year simulated daily time series of precipitation and potential evapotranspiration. The time series are representative of stationary climates for the periods 1961–1990 (“baseline”) and 2071–2100 (“future”). The time series of future climate were obtained by downscaling the results of eight regional climate model (RCM) experiments, driven by the SRES A2 emissions scenario, using change factors for a series of climate statistics and applying them to stochastic weather generator models. The time series are characterized by increased precipitation in winter, less precipitation in summer, and higher air temperatures (between 2 °C and 5 °C) throughout the year.

Future climate scenarios project higher evapotranspiration rates, more irrigation, less drainage, lower discharge rates and lower groundwater levels, due to increased evapotranspiration and a slowing down of the groundwater system. As a result, lower concentrations of Cd and Zn in surface water are projected. The reduced leaching of heavy metals, due to drying of the catchment, showed a positive impact on a limited aspect of surface water quality.

© 2011 Elsevier B.V. All rights reserved.

1. Introduction

Climate change impacts on water resources are among the most important problems facing hydrologists today as water resource management systems have historically been designed under the assumption of climate stationarity (Milly et al., 2008). Hydrological impacts are expected directly through changes in

precipitation, and indirectly due to changes in potential evaporation and transpiration due to atmospheric warming. These impacts may be manifest through changes in runoff, infiltration, stream flow, actual evapotranspiration, and groundwater recharge, and depend on the local hydrological system as well as the projected climate change. In addition to the hydrological effects, these changes may have an effect on water quality and ecology. Furthermore, human management of the system such as groundwater extraction and agricultural and irrigation practices further complicate the assessment of climate change impacts on water resources (EU, 2009).

* Corresponding author at: Lawrence Livermore National Laboratory, 7000 East Avenue, Livermore, CA 94550-9234, USA.

E-mail address: visser3@llnl.gov (A. Visser).

Assessing the impact of climate change on water resources is dependent on obtaining high resolution projections of temperature and precipitation for the area of interest. General circulation models (GCMs), used to simulate climate on a global scale (typically at a horizontal resolution of between 250 and 600 km), are unable to resolve atmospheric processes sufficiently to provide the robust simulations of climate necessary for hydrological models, except for continental scale impact studies (Arnell, 1999, 2004; Oki et al., 2003; Vörösmarty et al., 2000). Dynamic downscaling of GCM results by means of physically-based regional climate models (RCMs) provides more reliable and regionally differentiated projections of climate change (Fowler et al., 2007). However, while RCMs offer an improved representation of atmospheric processes and better represent surface topography due to their higher resolution (25–50 km) they are still unable to resolve important processes such as convection and cloud physics which must therefore be parameterised. RCM simulations therefore may still not provide output at the resolution necessary for robust hydrological simulation. Furthermore, individual model structures and parameterisations may lead to systematic errors or bias from present day climate. Generally, an additional downscaling and bias-correction procedure is therefore required for hydrological applications (Christensen et al., 2008). This step, known as statistical downscaling, can be achieved by a wide range of procedures which are summarized by Wilby and Wigley (1997) and Fowler et al. (2007). These methods include the use of stochastic rainfall simulators (Burton et al., 2008) and weather generators (e.g. Kilsby et al., 2007) to provide consistent temperature and precipitation time series. The development of downscaled climate simulations using this approach for the area examined here is described by Van Vliet et al. (in press).

The uncertainties in climate change hydrological impact studies derive from the emissions scenario, the climate model structure and the downscaling techniques used for projecting future climates, as well as the models used to simulate the impact on hydrology or water quality (Kay and Davies, 2008; Olesen et al., 2007). One way of addressing uncertainties in future climate projections is through the use of multi-model and multi-scenario ensembles to force the hydrological model. This enables future impact assessments to incorporate sources of uncertainty arising from climate model structure, giving insight into the reliability and robustness of the observed hydrological effects (Goderniaux et al., 2009; Graham et al., 2007; Hagemann and Jacob, 2007; Kyselý and Beranová, 2009; Van Roosmalen et al., 2010; Yu and Wang, 2009).

One such ensemble is provided by the EU FP5 project PRUDENCE (Christensen et al., 2007), which has been used in various hydrological studies (Blenkinsop and Fowler, 2007; Goderniaux et al., 2009; Graham et al., 2007; Mavromatis, 2009; Olesen et al., 2007; Van Roosmalen et al., 2010). These studies are either limited to climate change impacts on surface water systems (Fowler and Kilsby, 2007), specifically aimed at river flooding (Dankers and Feyen, 2009), droughts (Blenkinsop and Fowler, 2007; De Wit et al., 2007; Feyen and Dankers, 2009; Van Pelt et al., 2009) or suspended sediment transport (Thodsen et al., 2008). Some studies cover climate change impact on all aspects of the hydrological system including evapotranspiration (Kay and Davies, 2008), groundwater levels and ground-

water recharge (Bormann, 2009; Brouyère et al., 2004; Goderniaux et al., 2009; Scibek and Allen, 2006; Van Roosmalen et al., 2007; Wegehenkel and Kersebaum, 2009), irrigation (Ficklin et al., 2009, 2010), crop growth (Challinor et al., 2009; Mínguez et al., 2007) and the vegetation response (Brolsma et al., 2010; Wegehenkel, 2009).

While the potential impact of climate change on the quantitative aspects of hydrology has been well investigated, fewer studies have focussed on climate change impacts on water quality. So far, neither PRUDENCE simulations nor any other climate change scenario ensemble have been used to assess the impact of climate change on aspects of water quality. The existing water quality studies have followed various approaches, for example, recent dry years indicated, by proxy, a deterioration of several aspects of water quality of the Meuse River (Van Vliet and Zwolsman, 2008). Various water quality parameters have been studied for catchments across the UK by means of an integrated catchment model (Whitehead et al., 2009). Other studies have focused on specific aspects of water quality, such as nutrients (Darracq et al., 2005; Destouni and Darracq, 2009b; Park et al., 2010), nitrate (Futter et al., 2009; Olesen et al., 2007; Sjøeng et al., 2009; Wilby et al., 2006), phosphorous (Jennings et al., 2009), or pesticides (Bloomfield et al., 2006).

The impacts of climate change on heavy metal contamination have been discussed qualitatively for marine ecosystems (Schiedek et al., 2007). The potential increased risk of flooding due to climate change has implications for the inundation of contaminated land causing an increased risk of contaminants being remobilized in floodwater and of contaminated sediment and water reaching the freshwater and marine environment. The temperature dependence of arsenic release from flooded contaminated soils (Weber et al., 2010) is one mechanism that may cause climate change to have an impact on the release of heavy metal contamination. Furthermore, heavy metal contamination often accumulates in the topsoil and the contaminant leaching is therefore controlled by the location of the water table. This is especially the case in lowland areas such as the Keersop catchment. As a result, high concentrations of heavy metals in surface water are often found during periods with high groundwater levels and high discharge rates (Rozemeijer and Broers, 2007). In addition, total concentrations of heavy metals with high adsorption capacities to suspended solids also increase, due to increased resuspension of contaminated suspended sediment under high river discharge rates (De Weert et al., 2010; Jacoby, 1990; Mulholland et al., 1997).

The objective of this study is to assess the impact of climate change on the leaching of the pre-existing spatially extensive trace metal contamination and the concentrations in the surface water system. The Kempen area, on the border between The Netherlands and Belgium, is an example of a large-scale diffuse contamination with heavy metals that pose a threat to surface water quality. This heavy metal contamination, with Cd and Zn for example, has accumulated in the topsoil and leaches towards the surface water system by different pathways, namely overland flow and subsurface drainage, especially during periods with high groundwater levels and high discharge rates (Rozemeijer and Broers, 2007). The contamination of surface water due to leaching of contaminants already present and adsorbed to the soil on a

large-scale is sensitive to changes in the location and dynamics of the water table, drainage and stream discharge fluxes (Bonten et al., in preparation).

We focus on the Keersop, a 43 km² catchment located in the center of the Kempen area (Section 2.1). Because the leaching of heavy metals from soils to surface water is strongly related to water table fluctuations, studying the effect of climate change on water quality requires the modeling of hydrological processes with very short time steps to accurately simulate water table fluctuations.

Therefore, we used the numerical quasi-2D unsaturated zone Soil–Water–Atmosphere–Plant (SWAP) model (Section 2.2) which was constructed to assess the present day contamination of the Keersop stream with Cd and Zn. For this study, the model was driven by future climate scenarios and the results were compared to baseline climate model simulations. Future climate scenarios were derived by downscaling an ensemble of RCMs from the PRUDENCE project (Section 2.3). To assess the possible impact of climate change on Cd and Zn concentrations in surface water, we analyzed the projected changes in the water balance, groundwater levels and discharge rates of the Keersop catchment and the annual mass balances and (dissolved) concentrations of Cd and Zn in soil profiles and in the Keersop stream. The effects on the hydrology (Section 3.1) and contaminant transport (Section 3.2) are discussed and compared with recent climate change impact studies (Section 4) followed by the conclusions (Section 5).

2. Methods

2.1. Study area: hydrogeology, contamination history

The Keersop stream (51.3°N, 5.4°E) is a second-order tributary of the river Meuse, draining an intensive agricultural and heavily populated area (Pieterse et al., 2003). It is located in the Kempen (Fig. 1), a flat lowland area with surface levels increasing from about 20 m above sea level in the north to about 40 m above sea level in the south. Brook valleys are 10 m below the surrounding area at most; the maximum slopes are approximately 1%. The mean annual rainfall is 826 mm/yr and the reference evapotranspiration for grassland is 590 mm/yr. The geology consists of sand and loamy sand layers of Pleistocene

age (Van der Grift and Griffioen, 2008). The area was originally drained by a natural system of brooks and streams, but in the 19th century this natural system was extended with a fine network of ditches to form an interconnected surface water system and make agricultural land use possible. In the 20th century, tile drainage was installed in large parts of the agricultural land and now more than half of the study area is used for agriculture, most of which is drained by ditches and/or tile drainage (Van der Grift and Griffioen, 2008). Present day groundwater levels range from about 0.25 to 4.0 m below the soil surface. About 1/3 of the area has an average groundwater level that is within 1 m below the soil surface as well as an average highest groundwater level within 0.5 m below the soil surface.

From 1880 to 1974 the chimneys of four zinc ore smelters, using very polluting pyrometallurgic zinc refining procedures, emitted oxides of heavy metals that reached the soils in the Kempen area either by dry deposition or through rainfall. Besides the atmospheric emissions, heavy metals contaminated the area through zinc ash roads, severe groundwater pollution at the smelter sites and direct drainage from the smelter sites to surface water. While the zinc ash roads and the smelter sites caused intense line and point source contamination, the historic input of heavy metals on the soil through atmospheric deposition has resulted in an excessive accumulation in the topsoil in the Kempen region. The zinc ore smelters switched to an electrolytic process in 1974, but despite the cessation of direct emissions to the environment, soils and sediments still contain high metal concentrations and act as possible sources of metal pollution for the aquatic environment. Cd and Zn concentrations in the soil range from <0.2 mg/kg Cd and <20 mg/kg Zn at locations over 30 km from the smelters to 5.3 mg/kg Cd and 733 mg/kg Zn at a location within two km from the Budel smelter (Van der Grift and Griffioen, 2008). Because the accumulation of Cd and Zn is so widespread, leaching to the groundwater and surface water threatens water quality in the entire Kempen area. De Jonge et al. (2008) showed that the zinc concentrations in the Dommel, a small lowland river in this area, have impacted the macro-invertebrate community composition and diatom community structure.

Concentrations of Cd and Zn were monitored in the Keersop stream on a monthly basis from 1980 to 2000 and for Cd varied

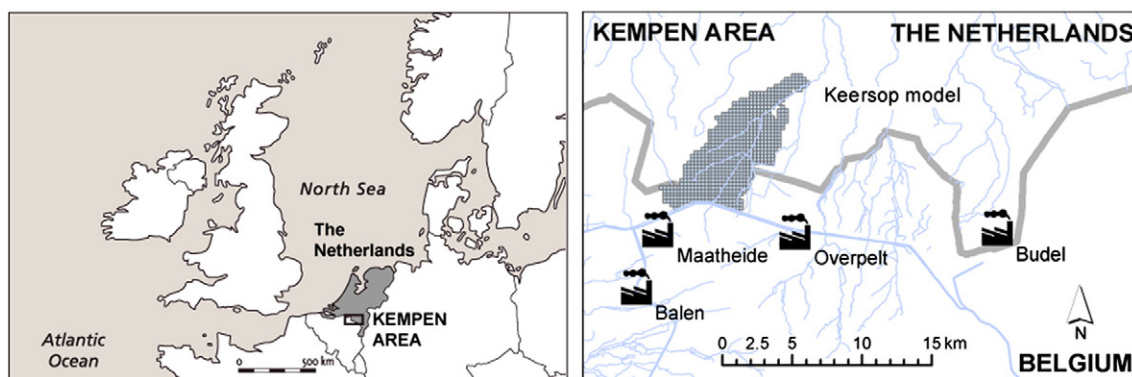


Fig. 1. Location of the Kempen area in Europe (left) and the Keersop model area (shaded) within the Kempen area with the surface water system (light blue lines), the Dutch-Belgian border (thick line), and the location of the four zinc ore smelters (right).

between 0.12 and 2 $\mu\text{g/l}$, while Zn concentrations varied between 10 and 440 $\mu\text{g/l}$. In comparison, the Dutch water quality threshold value is 0.4 $\mu\text{g/l}$ (dissolved) or 2 $\mu\text{g/l}$ (total, dissolved plus suspended) for Cd, and 9.4 $\mu\text{g/l}$ (dissolved) or 40 $\mu\text{g/l}$ (total) for Zn (<http://www.rivm.nl/rvs/>), which is similar to the EU maximum allowable concentration of up to 1.5 $\mu\text{g/l}$ Cd depending on water hardness classes (EU, 2008). The dissolved concentrations of Cd and Zn in the Keersop are related to groundwater levels and stream discharge rates (Kroes et al., 2008a) because Cd and Zn have accumulated in the topsoil. Therefore, the impact of climate change on groundwater levels and discharge rates is expected to impact the concentrations of Cd and Zn in the Keersop as well.

2.2. Hydrological and contaminant transport model

Climate change impacts on the hydrology and leaching of heavy metal contamination of the Keersop were investigated using the Soil–Water–Atmosphere–Plant model (SWAP v3.2, Kroes et al., 2008b, Fig. 2). The SWAP model is capable of simulating water, heat and solute fluxes in the soil, lateral drainage, and plant growth and transpiration. Because most transport in the root and vegetation zone occurs in the vertical, the SWAP model is 1D in principle. A pseudo 2D approach is implemented in SWAP to simulate the interaction between groundwater and surface water using lateral water and solute flow through the groundwater system (Groenendijk and Van den Eertwegh, 2004). Using this approach the contaminant

load to surface water of a catchment size study area can be simulated transiently with a single model with reasonable simulation times (Kroes et al., 2008b).

A detailed description of the model is given by Bonten et al. (in preparation). The following section is a brief description of the key aspects of the model. The study area was modeled using 686 1D models, each of which represented a 250×250 m area within the catchment (Kroes et al., 2009). The depths of the soil profiles should be such that the streamlines between groundwater and surface water are included in the schematization, because they describe the interaction between groundwater and surface water. In the Keersop catchment, groundwater flow occurs in the Sterksel aquifer. The lower boundary of the model was fixed at a depth of 13 m below the soil surface because the knowledge of the thickness of this formation was not sufficient to allow spatial variation (Bonten et al., in preparation; Kroes et al., 2008a). Each model consisted of 40 layers, with thicknesses ranging from 1 cm at the top, to 2 m at the bottom of the model, at 13 m below the surface.

Each 1D model received a flux as lower boundary condition that was derived from a regional 3D MODFLOW model (Kroes et al., 2008a; Van der Grift and Griffioen, 2008). The bottom boundary is fixed in time, but varies spatially. The upper boundary received daily meteorological data from station Eindhoven for a 30-year period 1971–2000 (Heijboer and Nellestijn, 2002).

The model input was provided on a daily basis, but the model internally chooses smaller time steps, between 0.2 and 10^{-7} day as necessary to ensure stable and accurate calculations with a water balance deviation of 0.001 cm or less per day.

The leaching of water and solutes from the soil profile was modeled through five drainage levels. Each drainage level corresponded to a different pathway through the unsaturated and saturated zone. Drainage fluxes, implemented as lateral sink/source terms, are distributed uniformly over depth resulting in a vertical flux that will decrease with depth. This results in a vertical travel time distribution in the profile that will increase disproportionately with depth and a differentiation in travel times between drainage water and vertical flow. For systems with large horizontal flow components (large aquifers) this approach is not favorable because it neglects the horizontal concentration gradient. For small scale systems it has advantages because distributed modelling with different grid-properties facilitates upscaling to a regional scale.

The travel times in the saturated zone were approximated by a mixing-cell approach, equivalent to the exponential model for travel times in groundwater (Vogel, 1967). The mean travel time of each mixing-cell model was derived from the volume of the drained part of the aquifer, largely determined by the spacing of the specific drainage type. Groundwater and dissolved heavy metals that leached from the 1D model into the surface water system immediately reached the outflow point. Additionally, the inlet of water from a canal at the upstream end of the Keersop was simulated at a constant rate of $0.15 \text{ m}^3/\text{s}$. The travel time in the surface water system and processes in the stream and streambed were not incorporated in the model. While increased resuspension of contaminated sediment under high river discharge rates is known to also increase total concentrations of heavy metals with high adsorption capacities to suspended solids (Jacoby, 1990; Mulholland et al., 1997), the effect of resuspension was not incorporated in this study.

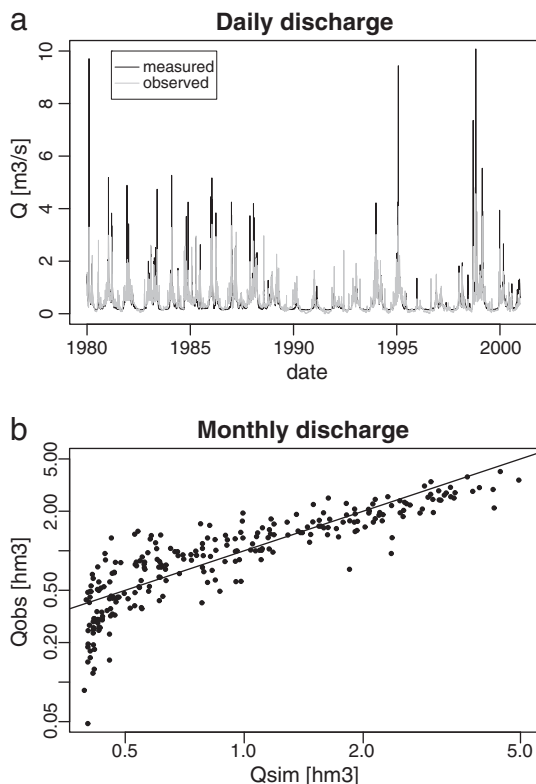


Fig. 2. Observed and simulated discharge at the outlet: daily time series (a) and monthly totals (b).

The model settings were based on the Dutch national scheme for parameterization of hydrological models (STONE, Van Bakel et al., 2008). Hydraulic soil properties were derived from the soil map of The Netherlands at the 1:50,000 scale, converted to soil hydraulic parameters according to the Dutch pedotransfer system Staring series (Kroon et al., 2001; Wösten, 1994). Chemical soil properties (clay and organic matter content, pH, Fe and Al hydroxide content) were assigned following Kroon et al. (2001). These parameters were necessary to simulate the sorption of Cd and Zn to soil sediments using Freundlich-type isotherms (Bonten and Groeneweg, 2008). Initial (pre-contamination) concentrations of Cd and Zn in the soils were derived from Bonten et al. (2008b).

Land use was classified into five natural types (natural grassland, heather, deciduous forest, pine forest, and Douglas fir) and three cultivated types (cultivated grassland, maize and arable land). Urban areas were classified as cultivated grassland. The irrigation of 44% of the area of cultivated land use types was simulated according to the STONE systematic (Van Bakel et al., 2008) whereby cropped land is irrigated when, at a depth of 20 cm below the soil surface, the pressure head drops below values of -316 , -500 or -200 cm for cultivated grassland, maize or arable land respectively. When the threshold value is exceeded, irrigation is applied which brings the root zone back to field capacity. The source of the water used for irrigation, either surface water or groundwater, is not explicitly considered in this study. For the analysis of the results, the eight land use types are grouped into natural land (37%), agricultural land (35%) and irrigated agricultural land (28%). The same land use and irrigation settings were used for the future climate simulations, thereby neglecting possible socio-economic adaptations to future climate. The results are therefore not predictions of future conditions, but provide projections of change in hydrology and contaminant transport solely due to projected climate changes.

The deposition of Cd and Zn on the soil surface was calculated using a regional mass balance approach (Van der Grift and Griffioen, 2008; Visser et al., 2007), distinguishing between land use types and proximity to the smelter. Three sources of Cd and Zn to the soil surface were considered: atmospheric deposition, manure and fertilizers, and leaching from zinc ash roads. Atmospheric deposition rates were obtained from Rozemeijer (2002) and Van der Grift and Griffioen (2008) and were related to the Budel smelter production, decreasing with distance from the smelters (Makasko et al., 1995). The contribution of manure and fertilizer use to the load of Cd and Zn was based on annual estimates of net heavy metal deposition from Statistics Netherlands (CBS, 2008) for the period 1980–2000. Deposition between 1950 and 1980 was based on (Van der Grift and Griffioen, 2008). The load in the period between 1880 and 1950 was assumed to increase linearly from one half to one times the load estimated for 1950. Zinc ash roads have been constructed since 1950 and the total area of zinc ash roads covers 0.55% of the catchment. The concentrations underneath these zinc ash roads were estimated to be 0.03 mg/l for Cd and 15 mg/l for Zn based on the monitoring information available, and the load for each specific 1D model was proportional to the area covered by zinc ash roads within the model footprint.

The Cd and Zn contamination in the model was initialized by running the model from 1880 to 2000 with historical

deposition. For this period the meteorological data observed between 1971 and 2000 were used repeatedly as a driving force. The purpose of this initial simulation was to produce consistent groundwater levels and soil moisture profiles and Cd and Zn concentration profiles in the soil, rather than test the sensitivity of the transport model to past climate changes, which was impossible because of the lack of reliable local meteorological data and historical measurements of Cd and Zn concentrations. As our results will show, climate change has little impact on the position of the contamination in the soil and using the 1971–2000 meteorological data is justified. For model validation, classified values of simulated and observed groundwater levels were compared. Groundwater levels were classified by first averaging the three highest (HG3) and lowest (LG3) bimonthly groundwater levels within a hydrological year. Secondly, the long-term mean high water (MHW) and mean low water (MLW) values were calculated as averages of at least eight annual HG3 and LG3 values. Long-term average groundwater levels were available for the Dutch part and for urban land (78% of the area). The comparison between observed and simulated MHW values was satisfactory with deviations of a few centimeters for shallow water tables; deviations increased with depth to MLW values with a maximum deviation of 45 cm below 1 m depth (Bonten et al., 2008a, in preparation; Kroes et al., 2008a). Discharge rates and Cd and Zn concentrations have been validated at the outflow point by comparison of results from the initialization period with a measured daily time series of discharge (Fig. 2a) and monthly totals (Fig. 2b). The model efficiency for monthly discharge predictions is 0.73 (Nash–Sutcliffe coefficient; (Nash and Sutcliffe, 1970)) and 0.36 for daily discharge predictions. Details of the validation procedures of the Cd and Zn concentrations are provided in (Bonten et al., 2008a, in preparation; Kroes et al., 2008a). The state of the Cd and Zn contamination after the year 2000 was validated to profiles of measured Cd and Zn concentrations in the study area, and then served as the initial conditions for the baseline and future climate scenarios.

2.3. Climate scenarios

The SWAP model was driven by 100-year long stochastic simulations of daily precipitation, air temperature and potential evapotranspiration, representative of a stationary climate for the periods 1961–1990 (“baseline”) and 2071–2100 (“future”). The time series were generated by the stochastic rainfall model Rainsim V3 (Burton et al., 2008) and the Climatic Research Unit (CRU) weather generator (Kilsby et al., 2007; Watts et al., 2004) by applying change factors (CF) (Prudhomme et al., 2002) derived from an ensemble of PRUDENCE RCM experiments. The generation of these time series is described in detail in Van Vliet et al. (in press).

2.3.1. Regional climate model (RCM) experiments

The PRUDENCE project (Christensen et al., 2007) provides a series of high-resolution simulations of European climate, primarily using the SRES A2 (medium-high) emissions scenario (Nakicenovic et al., 2000). To incorporate climate modeling uncertainty in future projections of change for the Keersop, the output of eight different RCM experiments from the PRUDENCE ensemble was used (Table 1). Details of the

eight individual experiments using six RCMs (Arpège, RACMO, RAO, REMO, HadRM3P, and HIRHAM) may be found in [Jacob et al. \(2007\)](#). Boundary conditions for this ensemble are derived primarily from the HadAM3H GCM ([Gordon et al., 2000](#); [Pope et al., 2000](#)). The HadRM3P and Arpège RCM simulations derive boundary conditions from HadAM3P and HadCM3 respectively. Both HadAM3H and HadAM3P are dynamically downscaled to an intermediate resolution from HadCM3 and are thus closely related and may be considered as the same GCM. Two experiments also use boundary conditions derived from the ECHAM4/OPYC coupled atmosphere–ocean model ([Roeckner et al., 1996](#)). The alternative acronyms used by the AquaTerra project ([Gerzabek et al., 2007](#)) are used throughout this paper, the suffix of each denoting the driving GCM.

It should be noted that this ensemble does not sample the full range of potential model uncertainty and model structure is sampled in neither a systematic nor random way. Many climate models possess similar or even identical parameterizations and algorithms and thus such ensembles do not constitute totally independent samples of the uncertainty space ([Collins, 2007](#)) but represent an “ensemble of opportunity” ([Tebaldi and Knutti, 2007](#)). Nonetheless, this study represents a significant advance in the study of the response of groundwater contamination and the same framework can readily be applied to a larger ensemble and different emissions scenarios.

2.3.2. Downscaling methodology

For each of the eight selected RCM experiments, mean daily air temperature and daily total precipitation for the baseline and future time periods were extracted from the two grid cells overlying the study area. These simulations were used to calculate change factors (CFs) for the future period relative to the baseline on a monthly basis for mean rainfall, proportion of dry days, daily rainfall variance, daily rainfall skewness, 1-day lag auto correlation, mean temperature and temperature variance as described in [Van Vliet et al. \(in press\)](#). These were, in turn, applied to the stochastic rainfall model and weather generator to generate simulations of weather variables for the projected future climates. As both the rainfall model and weather generator apply RCM-derived CFs to station scale data, this approach provides downscaled climate projections at a point scale through a two-stage process.

Firstly, the stochastic rainfall model RainSim V3 ([Burton et al., 2008](#)) was used to generate 100-year temporally stationary

climate as projected by application of the PRUDENCE ensemble CFs. RainSim was calibrated to the monthly characteristics of observed daily precipitation at the Lommel meteorological station (KMI-RMI; 51.24°N, 5.36°E) in Belgium for the baseline period. Average annual precipitation (1960–1989) at this station was 826 mm. The process for generating the simulations for the baseline and future climate time series is described in detail for multisite simulations for the Dommel catchment ([Van Vliet et al., in press](#)).

For the second stage, the CRU daily weather generator (hereafter abbreviated to CRU WG) was used to generate 100-year daily time series of potential evapotranspiration. The CRU WG uses regression relationships between precipitation and secondary variables comprising mean temperature, temperature range, vapor pressure, wind speed, and sunshine hours ([Kilsby et al., 2007](#)). Relative humidity and reference potential evapotranspiration (PET) are subsequently calculated from these; the latter using the Penman-Monteith method ([FAO, 1986](#)). The WG regression parameters were derived from daily observations of precipitation, precipitation, air temperature (minima and maxima), wind speed, vapor pressure and sunshine hours observed between 1985 and 2006 at the Eindhoven meteorological station (KNMI; 51.45°N, 5.41°E) in The Netherlands, located 10 km north of the catchment. Mean annual air temperature and calculated potential evapotranspiration at this station (1985–2006) were 10.2 °C and 672 mm. This station was selected because it offers a longer continuous series of homogeneous climate data than is available elsewhere near the study area and thus provides a statistically meaningful representation of inter-variable relationships for the observed climate. As the CRU WG is conditioned on the rainfall simulations generated by RainSim, it generates temporally consistent time series of weather variables to match the rainfall time series. Further details of the implementation of the CRU WG and its perturbation for future climates are presented in ([Kilsby et al., 2007](#)) and the WG model validation and application for the data applied here is provided by [Van Vliet et al., \(in press\)](#).

Before examining the hydrological impacts projected under these scenarios for 2071–2100, a brief analysis of the projected climatic changes was undertaken. The CFs for mean precipitation and mean temperature, indicating future change projected by the eight RCM experiments averaged over the two selected grid cells, show a strong seasonal variation, with highest air temperature increases during summer, a distinct increase in winter precipitation and a pronounced decrease in summer precipitation ([Fig. 3](#)). The downscaled precipitation scenarios across the Dommel catchment project an increase in mean daily precipitation of +9% (ARPEGE_H) to +40% (RCOA_E) and an increase in the proportion of wet days (precipitation > 1.0 mm) during winter ([Van Vliet et al., in press](#)). During summer however, a decrease in mean daily precipitation of –16% (REMO_H) to –57% (RCOA_E) is projected accompanied by a decrease in the proportion of wet days. Mean wet-day amount, a simple measure of precipitation intensity, is also projected to increase by most models, by up to 23% in winter (RCOA_E). The models also generally project an increase in mean wet-day amount in summer of up to 16% (RACMO_H) even though mean precipitation is projected to decrease during this season. Furthermore, the probability density functions of daily precipitation totals for the Lommel station (not shown) were consistent with this, indicating a projected increase in the

Table 1

The eight PRUDENCE project RCM experiments used in this study. The alternative acronyms used by the AquaTerra project ([Gerzabek et al., 2007](#)) are used throughout, the suffix of each denotes the driving GCM.

AQUATERRA ACRONYM	RCM	DRIVING GCM	PRUDENCE EXPERIMENT (baseline/future)
ARPEGE_H	Arpège	HadCM3 A2	DA9/DE6
RACMO_H	RACMO	HadAM3H A2	HC1/HA2
RCOA_E	RCOA	ECHAM4/OPYC A2	MPICL/MPIA2
RCOA_H	RCOA	HadAM3H A2	HCCTL/HCA2
REMO_H	REMO	HadAM3H A2	3003/3006
HAD_P_H	HadRM3P	HadAM3P A2	adeha/adhfa
HIRHAM_E	HIRHAM	ECHAM4/OPYC A2	ecctr1/ecscA2
HIRHAM_H	HIRHAM	HadAM3H A2	HC1/HS1

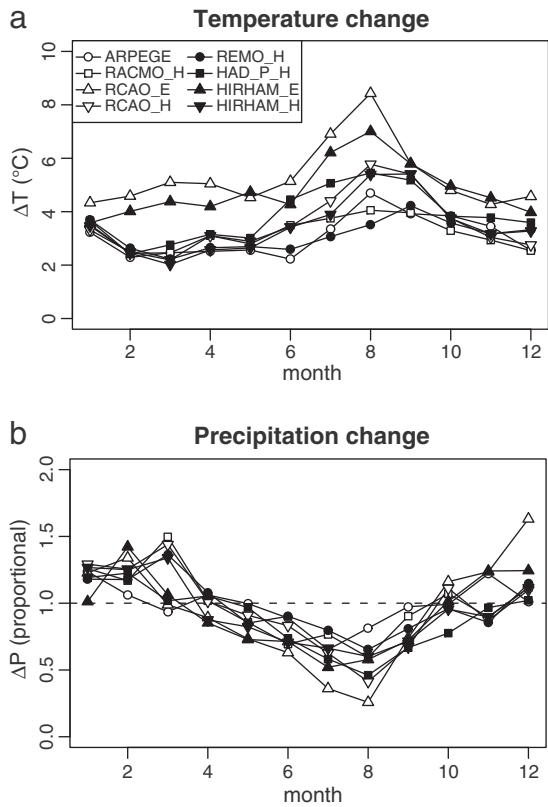


Fig. 3. Change factors of mean precipitation (a) and mean temperature (b), averaged for the two RCM grid cells overlying the meteorological stations in the Dommel catchment for the 8 selected RCM experiments.

probability of high daily totals under the future scenario relative to the baseline.

Projected mean winter temperatures for 2071–2100 range from 7.7 °C to 9.1 °C, while for summer the range is 19.9 °C–23.3 °C relative to mean winter and summer temperatures of 3.8 °C and 16.8 °C respectively for the baseline. Mean annual potential evapotranspiration for the Eindhoven station is projected to increase for all models, from 663 mm/yr to values ranging from 777 mm/yr (+17% for ARPEGE_H) to 904 mm/yr (+36% for RCAO_H), with the largest increases during the summer months. As indicated, the RCM ensemble projections shows consistency in the direction of seasonal changes but the individual experiments diverge in terms of the magnitude of projected climate changes. In a detailed consideration of the projected climate changes for the Dommel catchment from the PRUDENCE ensemble, Van Vliet et al. (in press) note that the downscaled climate projections are strongly influenced by the GCM used to provide boundary conditions for each RCM experiment.

2.4. Analysis

To test the hypothesis that variations in contaminant concentrations are related to groundwater level fluctuations, we first studied the relationship between simulated groundwater levels, stream discharge and concentrations of Cd and Zn in

discharged water for each of the land use classes under baseline climate. We specifically studied concentrations rather than contaminant mass fluxes to separate the effect of fluctuating discharge rates. To analyze the impact of land use, we aggregated the results for the entire catchment, as well as for the area of natural land, agricultural land and irrigated agricultural land. Secondly, to study climate change impacts on the hydrology we investigated the annual water balance and fluxes within the catchment, with emphasis on the potential and actual evaporation and transpiration, changes in groundwater levels and stream flow on a monthly basis. Thirdly, we investigated the climate change impact on contaminant transport and leaching by analyzing the average annual Cd and Zn mass balances and redistribution of Cd and Zn in the catchment, profiles of the concentrations of Cd and Zn in the soil before and after the baseline and future climate simulation period, and the concentrations of Cd and Zn in the Keersop stream on a monthly basis. We specifically analyze the concentrations of Cd and Zn, rather than mass loads, to distinguish between the climate change impacts on discharge rates and contaminant concentrations.

The differences between the results of the hydrological model driven by the baseline and future climate scenarios were interpreted as projections of changes in hydrology and contaminant concentrations under projected future climate, rather than predictions of future conditions or concentrations. Predictions of future conditions would require adjusting agricultural and irrigation practices to future socio-economic demands, as well as including climate feedbacks of such practices into the future climate projections. Although the irrigation rules imply a response to changing climate, this response is the same for both baseline and future climate scenarios. Therefore, our results merely present a direction of change and an estimated uncertainty range as a result of projected climate changes alone.

3. Results

3.1. Groundwater levels and contaminant concentrations

We studied various approaches to aggregate the groundwater levels that are simulated in each of 686 models on a daily basis, to monthly statistics representing the entire catchment or the different land use classes. We found that the best relationships with discharge rate and contaminant concentrations were obtained by first aggregating groundwater levels spatially and then temporally. Specifically, we first calculated the median groundwater level across the catchment (or land use class) on a daily basis and second calculated the 95th percentile of median groundwater levels within each month. This groundwater level statistic represents the monthly high groundwater level conditions for the catchment (of each of the land use classes) and it shows the following relations with discharge rates and Cd and Zn concentrations (Fig. 4). Discharge rates from the catchment increase if the groundwater level statistic increases above 1 m below surface (Fig. 4a–d). Natural land produces lower discharge rates, even at higher groundwater levels, while highest discharge rates are simulated from irrigated agricultural land. Concurrent with higher discharge rates, Cd and Zn concentrations in surface water are also higher during higher groundwater levels (Fig. 4e–l).

Although the relationships between discharge rate and groundwater level statistic are different for each of the land use

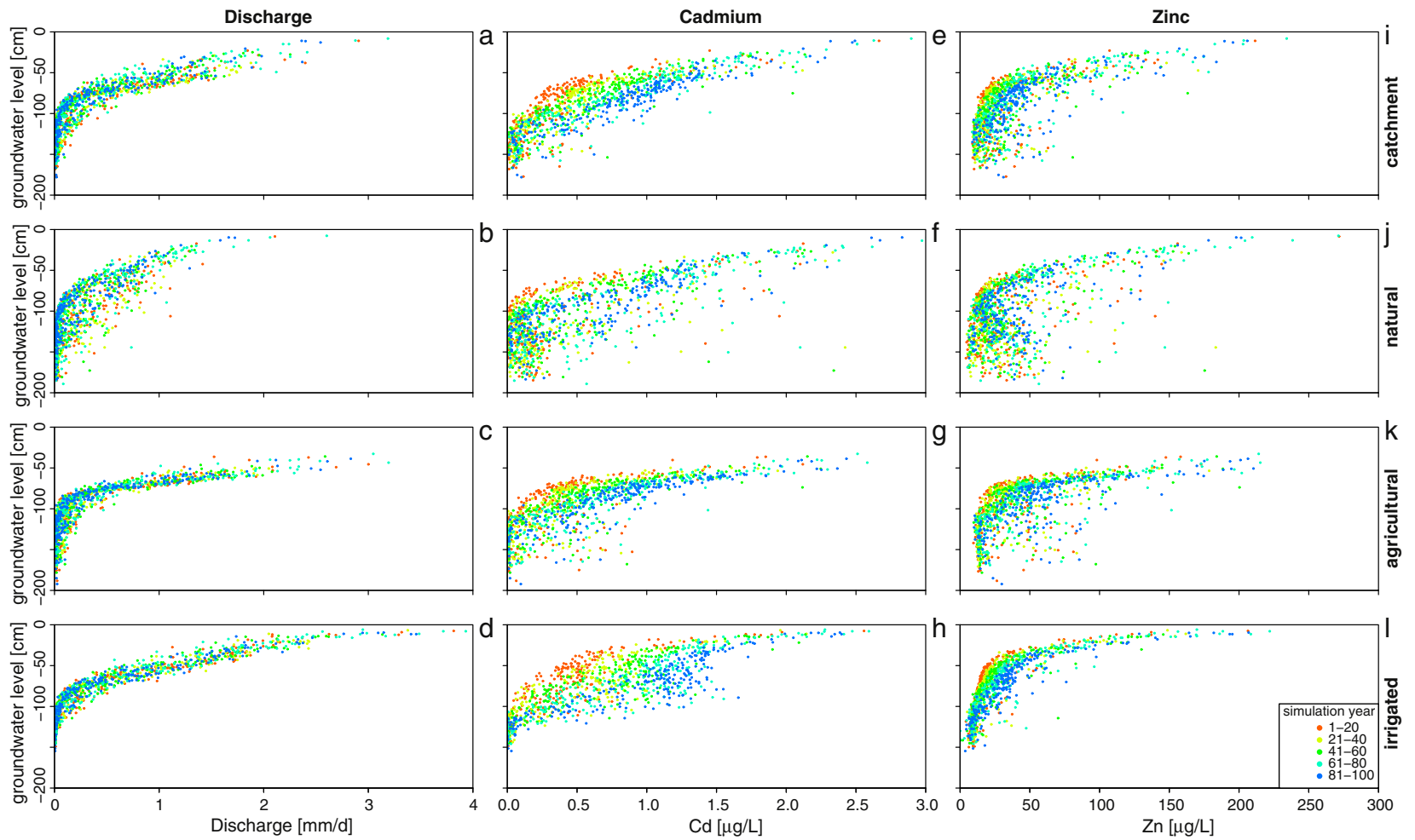


Fig. 4. Simulated discharge, cadmium and zinc concentrations versus the monthly 95th percentile of the spatial median groundwater level under baseline climate.

classes, they remain essentially the same throughout the simulated period. In contrast, the relationships between concentrations of Cd (Fig. 4e–h) and Zn (Fig. 4i–l) and the groundwater level statistic changed over the course of the simulated time period. Higher concentrations of Cd and Zn are projected for the same groundwater level at the end of the simulation period compared to the start of the period. This effect is due to the downward transport of Cd and Zn during the simulation period (see Section 3.2.3). This effect is particularly strong for Cd because it is transported further downward than Zn. It should be noted that although higher concentrations occur at lower groundwater levels near the end of the simulation period, discharge rates remain low at low groundwater levels, resulting in a less pronounced effect in the relationship between the mass load and the groundwater level. This effect shows that while the climate input is stationary and no trends may be determined within the 100 year period for the hydrological state of the system, the heavy metal contamination is not in a steady state and the response of the catchment to groundwater level variations in terms of contaminant concentrations is transient over time. The heavy metal contamination as it is present in the subsurface today will be transported by soil water and groundwater flow, both under the baseline and future climate projections.

3.2. Climate change impacts on hydrology

3.2.1. Climate change impacts on the annual water balance of the catchment

Under the baseline climate (1961–1990), the projected precipitation is 822 mm per year on average, which was close to the observed 826 mm/yr. In addition, irrigation was applied at a rate of 3 mm per year averaged over the entire catchment. Precipitation and irrigation, averaged over the entire catchment, were distributed between interception evaporation (83 mm), surface runoff (3 mm), soil evaporation (188 mm) and plant transpiration (343 mm), leaving 212 mm for recharge of the local and regional groundwater system. Of the 212 mm/yr recharge, 42 mm/yr is removed through the lower flux boundary to the regional groundwater system, leaving 169 mm/yr to be drained by the local groundwater system.

Future climate projections have several effects on the annual water balance of the Keersop catchment (Table 2). Mean annual precipitation in the form of rain decreases slightly by 4% to 773 mm/yr, averaged over the eight future climate projections. Individual projections of precipitation range between 730 mm/yr (HAD_P_H) and 813 mm/yr (REMO_H). Precipitation on frost days (maximum temperature below 0 °C) decreases on average by 83% to 3 mm/yr. In response to drier and warmer summers, present day irrigation rules increase artificial precipitation on average by 1088% to 36 mm/yr, averaged over the entire catchment. The absolute decrease in mean annual precipitation is almost compensated for in the model by the increase in mean annual irrigation, thus the resulting total annual precipitation only decreases by 2% from 825 mm/yr to 811 mm/yr.

Interception decreases by 15% to 70 mm/yr, while runoff decreases to only 0.5 mm/yr. In contrast, transpiration and evaporation increase by 19% and 8% respectively to 409 mm/yr and 204 mm/yr. To compensate for the increased rates of evapotranspiration, total groundwater recharge is projected to

decrease by 38% to 132 mm/yr. While the recharge towards the regional groundwater system, the bottom flux in the model, is kept at 40 mm/yr by the model setup, the drainage flux decreases by 46% on average to 92 mm/yr. This adversely affects the amount of discharge to the Keersop stream by local drainage systems.

3.2.2. Evapotranspiration

Under the baseline, the actual evaporation (Eact) for the entire catchment (Fig. 5a, large open circle) is 79% of the potential evaporation (Epot). Due to higher air temperatures, potential evaporation is expected to increase by 24%, but actual evaporation is expected to increase by only 8%. Under future climate scenarios, the actual evaporation is only 69% of potential evaporation on average, but a large scatter between the scenarios exists (63%–74%). Evaporation from natural land (Fig. 5a, squares) is noticeably lower than from agricultural land and shows a negative trend with increasing potential evaporation under future climate scenarios. Under the baseline, the actual transpiration (Tact) for the entire catchment (Fig. 5b, large open circle) is 97% of the potential transpiration (Tpot). The difference between potential and actual transpiration is smaller than for evaporation because capillary rise to the root zone provides water for transpiration. While actual transpiration under baseline climate scenarios was close to the potential transpiration for all land types (Fig. 5a, large open symbols), the actual transpiration under future climate scenarios is significantly below potential transpiration. Actual transpiration from the entire catchment (large solid circle) is 14% below potential transpiration and as much as 23% lower for natural land (solid upward triangle). This indicates that vegetation and crop growth will become more water-limited than at present. Irrigation maintained the transpiration flux from irrigated agricultural land (downward triangles) at 99% of potential under all future climate scenarios. Even though the Tact/Tpot ratio decreased substantially, the absolute amount of transpiration increased by 19% for the entire catchment and 35% for irrigated agriculture because of higher potential transpiration. The irrigation rules applied in the model (Van Bakel et al., 2008) assume unlimited water availability for irrigation, which may not be the case in reality. Consequently, the increase in actual transpiration will be limited if water availability is not unlimited. In summary, the total latent heat flux from the catchment increases by 11%.

A comparison of the water balances of different land use types under different climate scenarios (Fig. 6) reveals the effect of irrigation on the climate change impacts as well as the variation between the climate scenarios. The total input of water for the entire catchment (Fig. 6a, top half) will either increase or decrease depending on the climate scenario. While the annual amount of precipitation on natural and agricultural land (Fig. 6b and c) decreases under all scenarios (by 6% on average), irrigation (Fig. 6, top dark gray bar) actually increases the total water input by 8% (Fig. 6d). The anthropogenic-influenced hydrological response of irrigated land is markedly different from natural or agricultural land. The modeled irrigation rules aim to meet the potential transpiration. While the impact of climate change on the water balance of natural land is driven by the change in natural precipitation, the hydrological response to climate change on irrigated land is driven by the increased potential of transpiration and thus by the projected

Table 2

Water balance fluxes (mm/yr) under baseline (1961–1990) and future (2071–2100) climate scenarios. “Future climate” column represents the average over all eight future climate scenarios, “average change” represents change from baseline to average future climate results. Individual scenario results for comparison. Snow indicates precipitation on frost days. Epot and Eact stand for potential and actual evaporation, Tpot and Tact stand for potential and actual transpiration.

	Baseline	Future climate	Average change	ARPEGE	RACMO_H	RCAO_E	RCAO_H	REMO_H	HAD_P_H	HIRHAM_E	HIRHAM_H
Rain	807	773	−34 (−4%)	812	802	764	771	813	730	757	736
Snow	15	3	−12 (−82%)	2	3	0	2	2	1	1	11
Irrigation	3	36	+33 (+1088%)	19	29	62	37	19	37	46	35
Natural precipitation	822	776	−46 (−6%)	814	805	764	772	815	731	759	746
Total precipitation	825	811	−14 (−2%)	832	834	826	809	834	768	805	781
Interception	83	70	−13 (−15%)	76	73	64	70	76	67	66	72
Runoff	3	1	−2 (−81%)	0	0	1	0	0	0	1	1
Tpot	354	477	+123 (+35%)	438	463	535	481	441	482	505	472
Tact	343	409	+66 (+19%)	401	409	421	412	403	405	417	401
Epot	237	295	+58 (+24%)	278	289	321	294	283	292	310	293
Eact	188	204	+16 (+8%)	206	203	202	201	208	201	203	205
Tact/Tpot	97%	86%		92%	88%	79%	86%	91%	84%	82%	85%
Eact/Epot	79%	69%		74%	70%	63%	68%	73%	69%	66%	70%
Total evaporative flux	613	683	+70 (+11%)	683	684	687	683	687	673	686	679
Drainage	169	92	−77 (−46%)	111	111	98	90	110	65	82	70
Bottom flux	42	40	−2 (−6%)	41	42	43	40	41	36	40	37
Total recharge	212	132	−80 (−38%)	152	153	140	131	151	101	123	107
Evaporation as fraction of precipitation	74%	84%		82%	82%	83%	84%	82%	88%	85%	87%
Recharge as fraction of precipitation	26%	16%		18%	18%	17%	16%	18%	13%	15%	14%

increase in temperature. The variability of the hydrological response between the different climate experiments is larger for irrigated land, because the irrigation rules provide between 66 and 219 mm/yr artificial precipitation on irrigated land in response to projected increased temperatures (if the irrigation demand can be met) while the variation in projected natural precipitation ranges between 730 and 813 mm/yr.

The drainage flux (Fig. 6, bottom half) decreases due to the decreased precipitation rates and due to the increased evaporation and transpiration. The decrease in drainage flux from irrigated agricultural land (Fig. 6d) is, at −29%, much lower than the decrease of drainage from agricultural land (−55%, Fig. 6b) and natural land (−61%, Fig. 6c). However, if the irrigation water is drawn from the surface water system – most irrigated agriculture is close to surface water – then subtracting the irrigation flux from the drainage flux reveals that the net contribution of irrigated agriculture to the surface water decreases from 237 mm/yr under the baseline climate to 50 mm/yr under the future climate scenarios, a decrease of 69%.

3.2.3. Groundwater levels

Each of the 686 SWAP models calculates a groundwater level on a daily basis. To derive monthly statistics from the spatially distributed daily groundwater levels, first the daily median groundwater level was calculated for the entire catchment as well as for the three land use classes. Second, the 5th, 50th (median) and 95th percentile of median daily groundwater levels were calculated for each calendar month for baseline climate. Groundwater levels show a seasonal pattern under baseline conditions (Fig. 7a) with lower levels and a smaller 5th–95th percentile range in summer, and higher levels and a larger 5th–95th percentile range in winter. Groundwater levels under natural land are generally lower than catchment average and groundwater levels under

irrigated land are higher. Agricultural land closely follows the catchment seasonal trends. The monthly 95th percentiles of projected groundwater levels, to which discharge and contaminant concentrations show a strong relation, are lower for all future climate scenarios (Fig. 7b). The largest difference in this groundwater level statistic between baseline and future climate scenarios is projected for October and November. Groundwater levels recover in December and January, thanks in part to a projected increase of winter precipitation for some scenarios. Based on the projected changes in groundwater levels under future climate scenarios, the largest impacts in terms of discharge and contaminant concentrations are expected for October through December.

3.2.4. Discharge rates of the Keersop

Monthly mean discharge figures show typical seasonal patterns under the baseline climate (Fig. 8), with high discharge rates in the winter months (November–March) and low discharge rates in the summer months (April–October). The annual discharge of the Keersop stream decreases for all RCM experiments, by 26% to 46% relative to the baseline ($12 \times 10^6 \text{ m}^3/\text{yr}$). While precipitation rates in winter are projected to increase (Fig. 3b), the decline in groundwater levels during summer months causes lower discharge rates throughout the fall and winter, by as much as 73% in December (HAD_P_H, Fig. 8b). Natural discharge during summer months (June–September) decreases to almost zero and stream discharge is maintained by the water inlet from an upstream canal. Comparing discharge rates during summer months to irrigation demands, shows that natural discharge and present day water inlet rates cannot meet irrigation demands under all future climate scenarios. This demonstrates that present day irrigation rules are most likely not sustainable under future climate change.

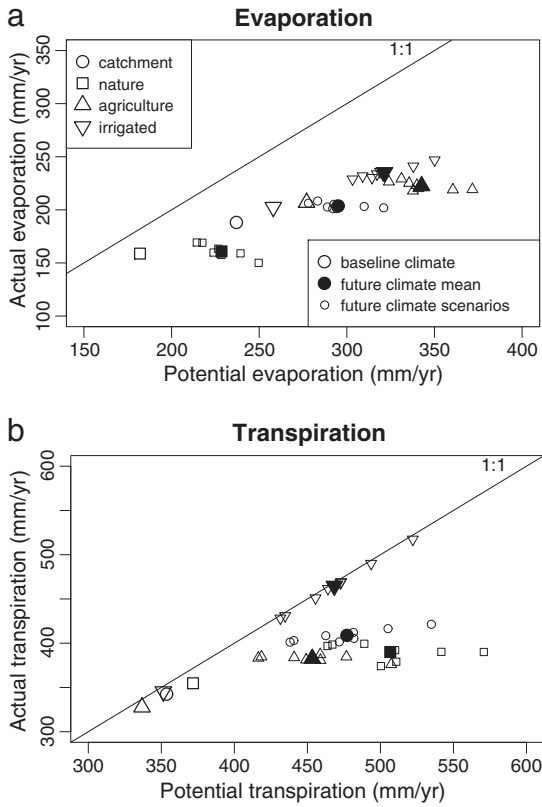


Fig. 5. Potential and actual evaporation and transpiration rates for natural land, agriculture and irrigated agriculture and the entire catchment average under baseline and future climate scenarios.

In summary, the projected impact of climate change on the hydrology of the Keersop catchment involves a shift from recharge and drainage towards more evaporation and transpiration. As such, groundwater flow in the catchment slows down.

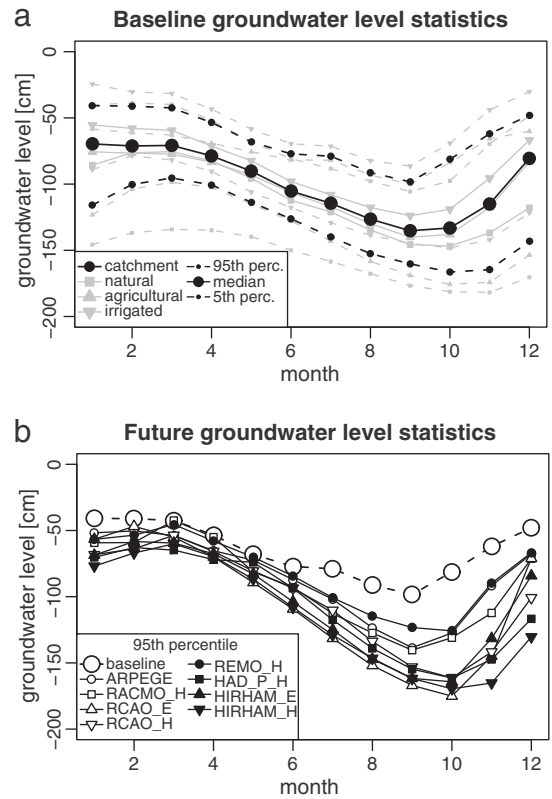


Fig. 7. Monthly statistics of the spatial median of simulated groundwater levels under baseline climate (a) and the projected monthly 95th percentiles under future climate scenarios (b).

3.3. Climate change impacts on contaminant transport

To differentiate between climate change effects and autonomous transport over the simulated time period, we will next

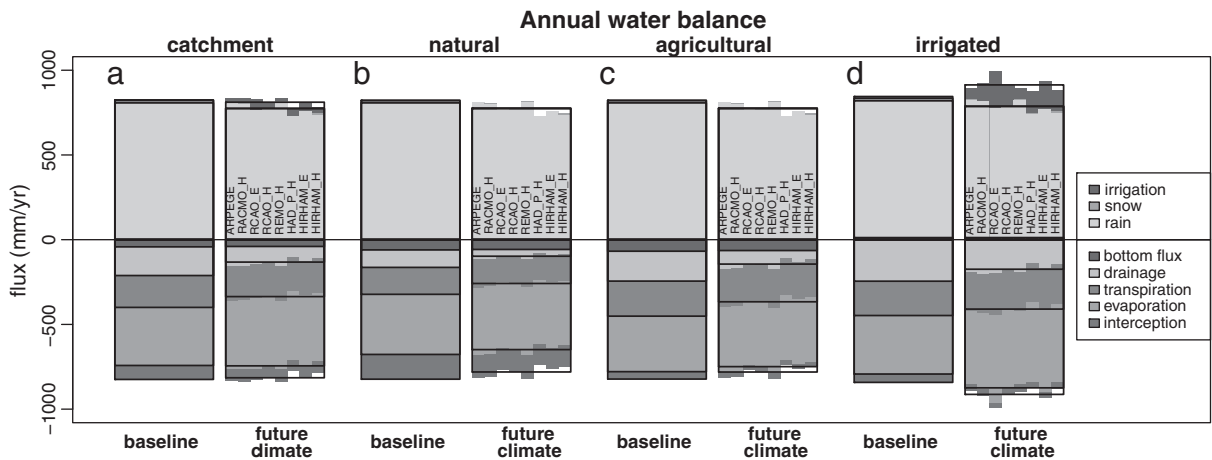


Fig. 6. Annual water balances for the entire catchment, natural land, rain-fed agricultural land and irrigated agricultural land, under baseline and future climate scenarios. Black boxes indicate the mean of the eight future climate scenarios.

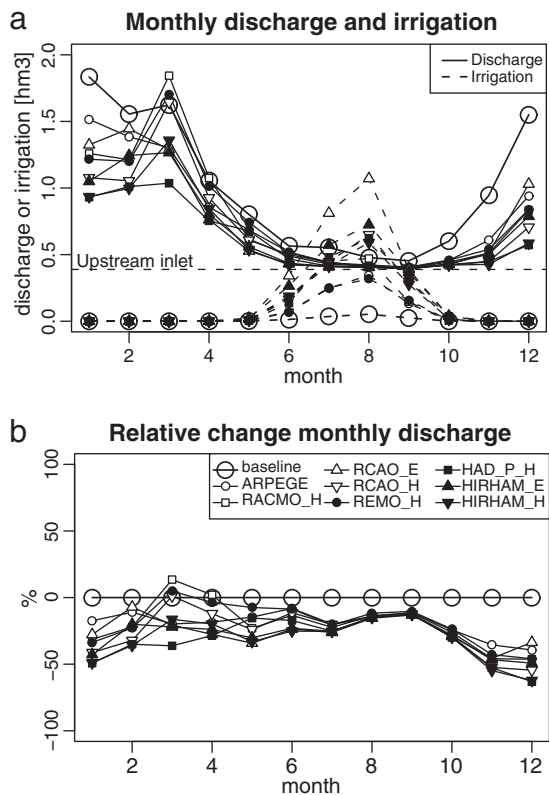


Fig. 8. Monthly discharge (solid lines) and irrigation (dashed lines) (a) and relative change of monthly discharge (b) of the Keersop stream, for the baseline scenario and eight future climate scenarios.

compare the mass balances and movement of the Cd and Zn contamination under future climate scenarios with those under the baseline climate.

3.3.1. Mass balance of contaminants

The initial stock of Cd and Zn averaged over the entire catchment is 1700 and 234,000 mg/m² respectively, while the annual input of Cd and Zn from atmospheric deposition, manure, fertilizer and the leaching of ash roads delivers 0.57 and 218 mg/m²/yr (Fig. 9). Under the baseline climate scenario, 33% of the annual Cd input (Fig. 9a) and only 6% of the annual Zn input (Fig. 9e) is removed by drainage, while the majority of the input (66% and 94%) is sorbed and stored in the soil profile, increasing the stock of Cd and Zn in the catchment by 2% and 9% over the 100 year simulation period. Under baseline climate, the catchment acts as a sink for Cd and Zn and the contamination is contained in the top soil. Under future climate scenarios, the drainage flux of Cd and Zn decreases to half of the baseline flux and only 16% and 3% of the annual input is removed from the catchment (Fig. 9a and e), respectively. The remainder accumulates in the subsurface. The effect on the total stock of Cd and Zn is negligible because it increases by 3% and 9% respectively over the 100 year future climate simulation period, compared to 2% and 9% for the baseline. Under both baseline and future climate scenarios, the contamination of the catchment increases in terms of the total amount of contaminant within the catchment. Fig. 9

also shows that while differences between the RCM experiments for the A2 scenario exist, the differences between land use types (Fig. 9b, c, and d; and f, g and h) are more significant.

3.3.2. Vertical profiles of average contaminant concentrations in the soil

The limited impact of climate change on the transport of Cd and Zn in the subsurface is illustrated by the average vertical profiles of concentrations for different land use types (Fig. 10), and a comparison between the start of the simulation period and the progression under baseline climate and future climate scenarios. The initial vertical Cd profile, averaged over all model cells in the catchment, showed a peak of 20 µg/l at 45 cm below the surface (Fig. 10a). The profile under natural land (Fig. 10b) shows higher concentrations, up to 29 µg/l at 55 cm into the soil, compared to the profile under agriculture (Fig. 10c) or irrigated agriculture (Fig. 10d). For the 100 year simulation period under baseline climate, the peak in the catchment average profile decreases to 11 µg/l while progressing to 80 cm below surface. A similar pattern is observed in the vertical Zn profiles. The initial vertical Zn profile for the entire catchment showed a peak of 1.7 mg/l at only 30 cm below the surface (Fig. 10e). Like the Cd profile, the Zn profile under natural land (Fig. 10f) shows higher concentrations, up to 2.3 mg/l at 35 cm into the soil. Over the course of the baseline climate simulation, the peak in the catchment average profile decreases to 1.3 mg/l while progressing to 45 cm below surface. Under natural land, the Zn peak concentration decreases by 40% to 1.5 mg/l, while peak concentrations under agricultural land decrease negligibly. This shows that while the historical contamination from the smelters is reduced under natural land, the deposition of Zn on agricultural land and the different sorption properties of agricultural soils sustain the Zn contamination.

The average profiles of average concentrations under future climate scenarios all show that the impact of climate change is minimal. Although a slightly increased retardation of the downward movement of Cd and Zn compared to baseline results can be seen, this effect is negligible compared to the differences between the initial and final profiles or the different land use classes.

3.3.3. Contaminant concentrations in the Keersop stream

Because Cd and Zn have accumulated in the top soil (Kroes et al., 2009), the concentrations in the Keersop stream under present day climate react to groundwater level fluctuations and show the same patterns as monthly discharge (Rozemeijer and Broers, 2007): high concentrations in December to May, and lower concentrations in June to November. (Fig. 11)

The concentrations of Cd and Zn in surface water are projected to decrease under the future climate scenarios. Small changes from baseline concentrations and little variability between scenarios are projected during summer months when Cd and Zn concentrations are low. The decrease in Cd and Zn concentrations is strongest in autumn and early winter, when groundwater levels are still low due to increased evapotranspiration during summer. Winter months, when concentrations are typically highest, also exhibit large variation between climate scenario results. Heavy precipitation events in March projected by the RACMO_H, RCAO_H and REMO_H scenarios can cause concentrations as high as baseline values for Cd and even higher than baseline for Zn.

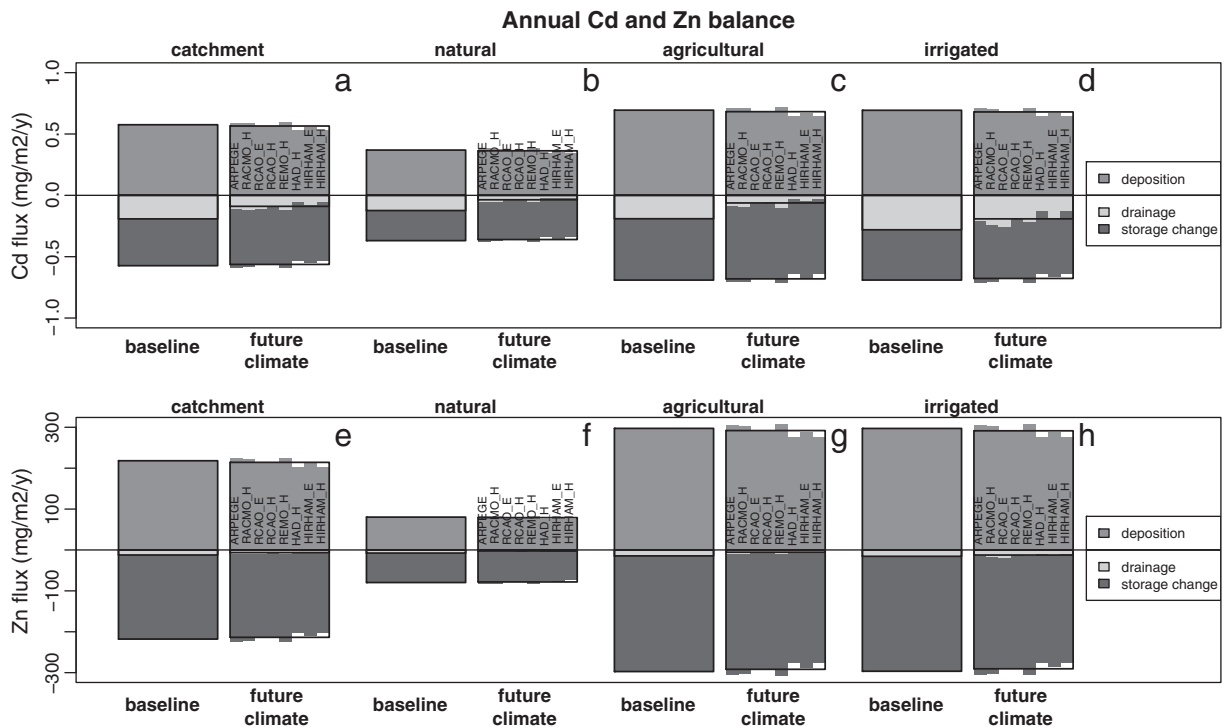


Fig. 9. Mass balances of Cd and Zn for the entire catchment, natural land, rain-fed agricultural land and irrigated agricultural land, under baseline and future climate scenarios. The black boxes indicate the mean of the eight future climate scenarios.

4. Discussion

For the Keersop, the impacts of climate change on hydrology are expected to manifest as increased irrigation and evaporation and a slowing down of the groundwater flow system. While annual mean precipitation decreases only slightly, the increased transpiration by plants increases the water flux from the soil to the atmosphere. This leads to a smaller proportion of the precipitation being routed to the groundwater system. The latter effect will increase the travel times in the groundwater system and in general the transport of contaminants in relation to the travel time (Van der Velde et al., 2010; Visser et al., 2009).

Regional climate change impact studies in Denmark (e.g. Onuşuel Gül and Rosbjerg, 2010; Van Roosmalen et al., 2007) have also projected increases in evapotranspiration and irrigation due to higher temperatures, but these have projected only a small increase in discharge and higher groundwater levels under increased annual precipitation. Contrary to the projected impacts in the Keersop area, a decrease of actual evapotranspiration is projected for Germany under climate change (Bormann, 2009), by including the adaptation of vegetation (Wegehenkel, 2009). However, the increase in low-flow days and decrease in groundwater recharge projected under climate change in north-east Germany (Wegehenkel and Kersebaum, 2009) are similar to our results. This demonstrates that the impacts of climate change on hydrology are likely to be highly spatially variable and highlights the importance of high resolution dynamical downscaling of GCMs to enable regional climate change impacts to be assessed (Hagemann and Jacob,

2007). For local climate change impact assessments, an additional statistical downscaling approach can be undertaken (Fowler et al., 2007; Van Vliet et al., in press).

The fixed bottom flux in the 1D models implies that regional groundwater hydrology is not affected by climate change. This is one of the limitations of the 1D ensemble model approach. Simulating the effect of climate change on regional groundwater hydrology would require a coupled model (e.g. Goderniaux et al., 2009) which was beyond the scope of this study. The choice for this approach is justified here because the SWAP model has the capability to accurately simulate capillary rise by the unsaturated zone in dry periods. This is essential because changes in evaporation and transpiration are not only determined by the changing patterns of precipitation and potential evapotranspiration, but also by the availability of soil moisture in summer.

Climate change impacts on hydrology can induce shifts in agricultural practices or production towards more warmth and drought resistant crops (Jennings et al., 2009; Mínguez et al., 2007) while elevated CO_2 concentrations have an effect on the actual transpiration of plants (Van Roosmalen et al., 2010). Increased CO_2 concentrations and changes in vegetation patterns and ecosystem adaptation towards more drought resistant plant communities were found to limit the increase in transpiration in a theoretical vegetated hill slope under the same precipitation scenarios as used in this study (Brolsma et al., 2010). This effect has, however, not been studied considering the actual topography and vegetation of the catchment. In general, vegetation response and elevated CO_2 concentrations appear to limit the increase in transpiration.

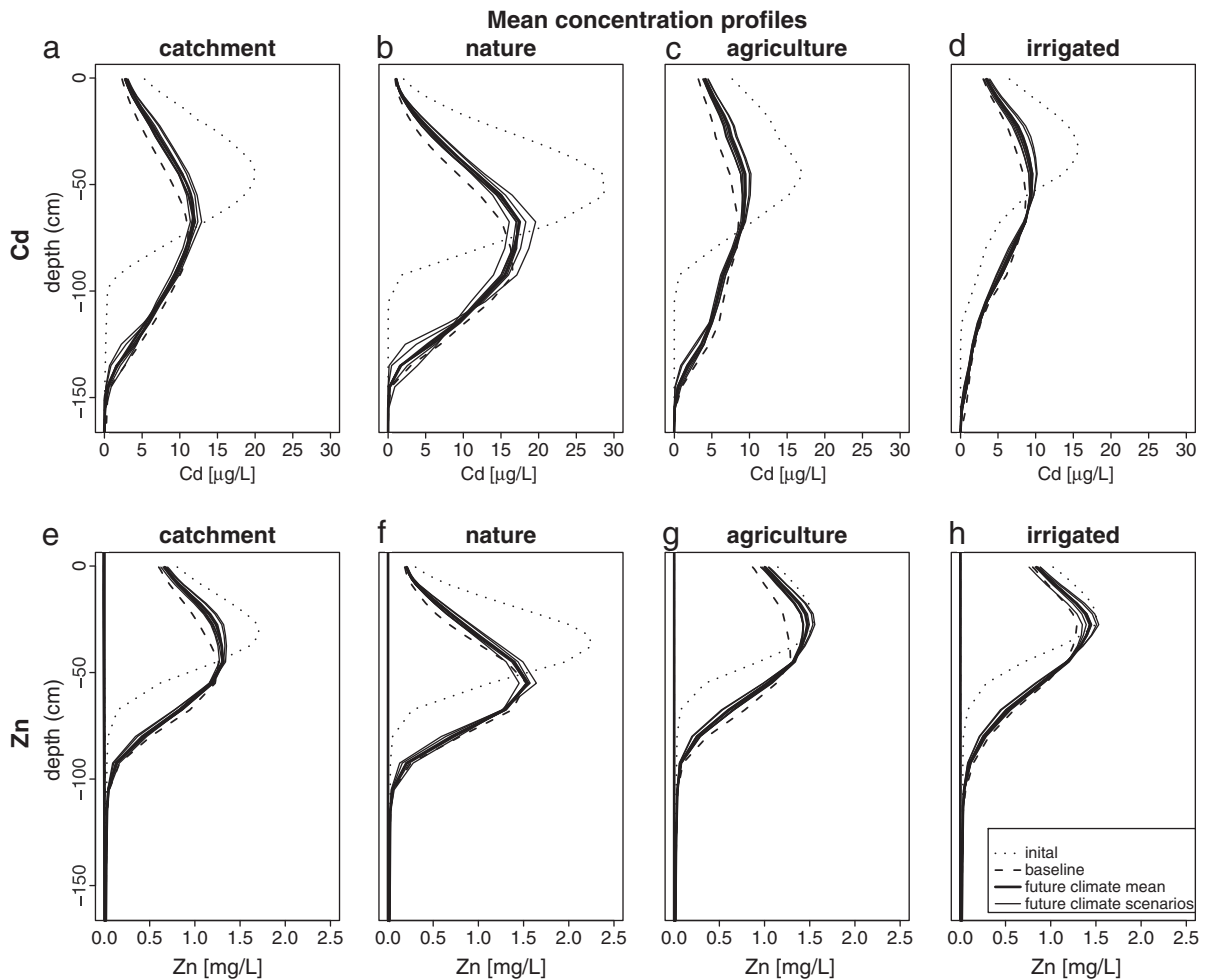


Fig. 10. Vertical profiles of Cd (a–d) and Zn (e–h) concentrations for the entire catchment (a,e), natural land (b,f), rain-fed agricultural land (c,g) and irrigated agricultural land (d,h), at start (initial), and at the end of the simulation period after 100 yrs of baseline climate and the eight individual future climate scenarios, as well as the mean of future climate scenarios.

It is acknowledged that changes in irrigation influence land–atmosphere interaction through feedbacks between soil moisture and land surface fluxes which in turn influence boundary layer conditions and regional climate. Previous studies have demonstrated that changes in irrigation (or land use changes in general) may affect meteorological conditions, particularly rainfall, cloudiness, humidity and air temperature (e.g. Ek and Holtslag, 2004; Koster et al., 2004; Wang et al., 2007) through changes in evapotranspiration and associated latent heat flux (Asokan et al., 2010; Destouni et al., 2010; Lobell et al., 2009; Shibuo et al., 2007). However, the climate response is complex; Boucher et al. (2004) identified an overall positive radiative forcing arising from increased water vapor but a potential negative climate sensitivity arising from evaporative cooling at the surface. Furthermore, vegetation changes associated with increased irrigation are also likely to further modify land–atmosphere interaction. The impacts of such land–atmosphere feedbacks on evaporative demand and precipitation are not accounted for in this study, as this would require fully coupled land surface–atmosphere modeling,

which is outside the scope of this study. Before this can be undertaken, more work is needed to quantify the scope and magnitude of land–atmosphere feedbacks in specific regions or catchments (Ferguson and Maxwell, 2011). Given these limitations, this study shows a strong impact of irrigation on the water balance of irrigated land under a moderate climate. Ficklin et al. (2009, 2010) found groundwater recharge to be very sensitive to climate change in an irrigated Mediterranean setting. Whether water is available for irrigation from surface water and whether present day irrigation is sustainable depends on whether the projected changes in the occurrence of low flow conditions in the Meuse under future climate (Van Pelt et al., 2009) are able to maintain the inlet of water to the Keersop catchment. The question is whether the Keersop can meet ecological and societal needs for freshwater (Baron et al., 2002) while agro-economical stakes will compete with environmental flow requirements (Gül et al., 2010). These questions relate to the socio-economic responses to climate change, which were beyond the scope of our study. Testing this feedback would require a regional or

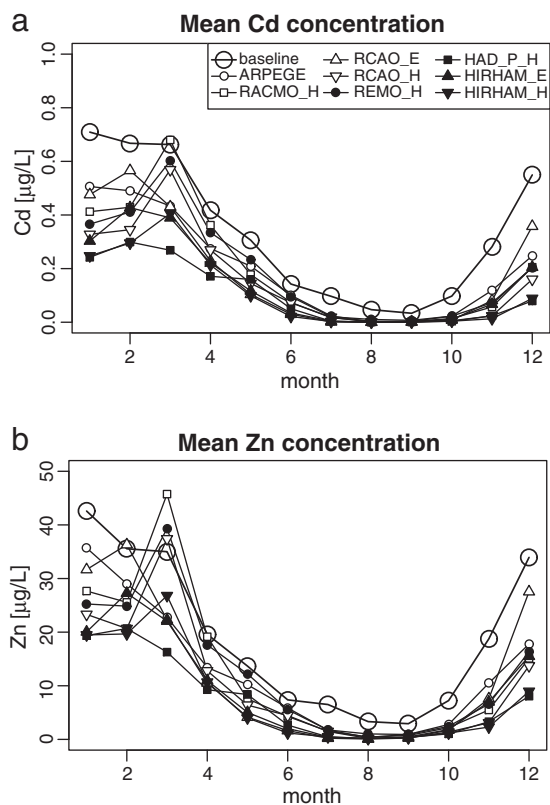


Fig. 11. Monthly mean Cd (a) and Zn (b) concentrations in the Keersop stream, for the baseline scenario and eight future climate scenarios.

continental scale coupled climate-hydrology-socio-economic model.

Climate change impacts on annual Cd and Zn mass balances and the concentrations in the soil are limited. These results are similar to the projected impacts of climate change on the transport and leaching of nutrients in Sweden (Destouni and Darracq, 2009a), although increased leaching of phosphorus was found under future climate scenarios predicting higher flow conditions (Jennings et al., 2009). In our study, climate change has a strong effect on concentrations of Cd and Zn in surface water, because the projected lower groundwater tables keep the saturated zone below the upper contaminated soil zone, limiting the transport of contaminants by short drainage paths such as shallow tile drains. The direct effects of increased temperature on sorption and desorption kinetics (Weber et al., 2010) was not studied here, because these are not expected in terrestrial soils. Increased resuspension of contaminated suspended sediment under high river discharge rates (De Weert et al., 2010; Jacoby, 1990; Mulholland et al., 1997) is also known to increase total concentrations of heavy metals with high adsorption capacities to suspended solids. While high discharge events under future climate scenarios in March and April are already expected to increase the dissolved concentrations of Cd and Zn, the effect of resuspension was not incorporated in this study. In general, comparisons of climate change impacts on contaminant transport and water quality are complicated because of the regional differences in future climate scenarios and the limited number of studies that have

specifically addressed the impacts of climate change on contaminant transport and leaching of heavy metals. While variation between projected effects from different future climate scenarios further complicate these comparisons, they also demonstrate the need for multi-model ensembles of climate change projections for reliable advice to water management (EU, 2009).

This study also showed that while the impact of climate change on the Cd and Zn concentrations in surface water is pronounced, the impact on the vertical profiles of Cd and Zn concentrations in the soil is minor compared to the impact of 100 year downward transport under continuous source inputs. This indicates the importance of accurately simulating the impact of climate change on soil moisture and groundwater levels, because these control shallow transport routes in lowland catchments and thereby stream concentrations, rather than changing sorption kinetics. The concentrations of Cd and Zn in our study area also vary with changing monthly discharge, in contrast to studies discussing chemostasis of concentrations of waterborne contaminants (in essence invariability of concentrations under variable flow conditions (Basu et al., 2011)). The simulated variations of Cd and Zn concentrations in response to groundwater level fluctuations are in agreement with observations of Cd and Zn from tile drains in a small lowland catchment in the east of The Netherlands (Rozemeijer et al., 2010). Our study also projected a different response for irrigated agriculture as opposed to natural and non-irrigated agricultural land, emphasizing the importance of using process-based models. Also, it is worth noting that even if a stationary future climate is assumed, transport processes are most likely not in a steady state and will play out on longer time scales.

5. Conclusions

Future climate scenarios project lower precipitation rates on a mean annual basis, but increased rates for winter months for the study area. On the other hand, both evaporation and transpiration fluxes increase, due to rising air temperatures. This increase is compensated for by a decrease in the drainage flux and groundwater recharge. As a result, groundwater levels decline and the annual discharge of the Keersop stream decreases under all future climate scenarios, by 26% to 46%. In conclusion, climate change leads to an intensification of irrigation practices, lower groundwater levels due to increased evapotranspiration and a slowing-down of the groundwater system.

Climate change leads to lower Cd and Zn concentrations for most of the year as a result of lower groundwater levels. Combined with lower discharge rates, the decrease of Cd and Zn mass loads through the surface water system is even more pronounced. This is in accordance with the predicted and observed response of solute transport to drier conditions (Rozemeijer and Broers, 2007; Rozemeijer et al., 2010) and the observed changes in total concentration of some heavy metals (i.e. lead, chrome, mercury and cadmium) under low flow conditions (Van Vliet and Zwolsman, 2008).

Thanks to the drier conditions projected for future climate a positive impact of climate change is projected on a limited aspect of surface water quality. The contamination of the subsurface is sustained and Cd and Zn will further accumulate,

but it will pose a smaller threat to surface water ecosystems under future climate conditions. This study shows for the first time the feasibility of transient simulation of contaminant transport through the soil and groundwater system driven by the PRUDENCE ensemble of future climate scenarios. Further, to provide useful advice to water managers on the impact of future climate on water quality, all aspects of water quality should be considered.

Acknowledgments

RCM data were obtained from the PRUDENCE project archive (<http://prudence.dmi.dk/>) which was supported by EU contract EVK2-CT2001-00132. This work was supported by the European Union FP6 Integrated Project AquaTerra (Project no. 505428) under the thematic priority sustainable development, global change and ecosystems. Dr. Hayley Fowler was supported by NERC Postdoctoral Fellowship award (2006–2010) NE/D009588/1. Luc Bonten and Bas van der Grift are thanked for the initial contaminant transport modeling. Aidan Burton of Newcastle University is greatly acknowledged for his work on the generation of future climate scenarios. Part of this work performed under the auspices of the U.S. Department of Energy by Lawrence Livermore National Laboratory under Contract DE-AC52-07NA27344. We would like to thank two anonymous reviewers for their helpful and constructive comments that helped us to improve the manuscript.

References

- Arnell, N.W., 1999. The effect of climate change on hydrological regimes in Europe: a continental perspective. *Global Environmental Change* 9 (1), 5–23.
- Arnell, N.W., 2004. Climate change and global water resources: SRES emissions and socio-economic scenarios. *Global Environmental Change* 14 (1), 31–52.
- Asokan, S.M., Jarsjö, J., Destouni, G., 2010. Vapor flux by evapotranspiration: effects of changes in climate, land use, and water use. *Journal of Geophysical Research* 115 (D24), D24102.
- Baron, J.S., LeRoy Poff, N., Angermeier, P.L., Dahm, C.N., Gleick, P.H., Hairston Jr., N.G., Jackson, R.B., Johnston, C.A., Richter, B.D., Steinman, A.D., 2002. Meeting ecological and societal needs for freshwater. *Ecological Applications* 12 (5), 1247–1260.
- Basu, N.B., Destouni, G., Jawitz, J.W., Thompson, S.E., Loukinova, N.V., Darracq, A., Zanardo, S., Yaeger, M., Sivapalan, M., Rinaldo, A., Rao, P.S.C., 2011. Nutrient loads exported from managed catchments reveal emergent biogeochemical stationarity. *Geophysical Research Letters* 37 (23), L23404.
- Blenkinsop, S., Fowler, H.J., 2007. Changes in drought frequency, severity and duration for the British Isles projected by the PRUDENCE regional climate models. *Journal of Hydrology* 342 (1–2), 50–71.
- Bloomfield, J.P., Williams, R.J., Goody, D.C., Cape, J.N., Guha, P., 2006. Impacts of climate change on the fate and behaviour of pesticides in surface and groundwater—a UK perspective. *The Science of the Total Environment* 369 (1–3), 163–177.
- Bonten, L.T.C., Groenendijk, J.E., 2008. Leaching of heavy metals from soils in rural areas. *Alterra-report 1695*. Alterra, Wageningen, the Netherlands. (in Dutch).
- Bonten, L.T.C., Kroes, J.G., Groenendijk, P., 2008a. Groundwater and surface-water contamination from diffusively contaminated soils. A case study: the Keersop catchment in the Kempen area. In: Luo, Y.M., McGrath, S.P., Newman, L., Wong, M.H., Mench, M., Japenga, J., Zhao, F.J., Vaněk, T., Doelman, P., Tagagi, K. (Eds.), *International Conference on Soil Remediation (SOILREM 2008)*, Nanjing, pp. 13–14.
- Bonten, L.T.C., Van der Grift, B., Klein, J., 2008b. Background Load in Surface Water of Heavy Metals Leaching from Soils Alterra-report 1636. Alterra, Wageningen, the Netherlands. (in Dutch).
- Bonten, L.T.C., Kroes, J.G., Groenendijk, P. and Grift, B.v.d., in preparation. Modelling diffusive Cd and Zn contaminant emissions from soils to surface waters.
- Bormann, H., 2009. Analysis of possible impacts of climate change on the hydrological regimes of different regions in Germany. *Advances in Geosciences* 21, 3–11.
- Boucher, O., Myhre, G., Myhre, A., 2004. Direct human influence of irrigation on atmospheric water vapour and climate. *Climate Dynamics* 22 (6), 597–603.
- Brolsma, R.J., van Vliet, M.T.H., Bierkens, M.F.P., 2010. Climate change impact on a groundwater-influenced hillslope ecosystem. *Water Resources Research* 46 (11), W11503.
- Brouyère, S., Carabin, G., Dassargues, A., 2004. Climate change impacts on groundwater resources: modelled deficits in a chalky aquifer, Geer basin, Belgium. *Hydrogeology Journal* 12 (2), 123.
- Burton, A., Kilsby, C.G., Fowler, H.J., Cowpertwait, P.S.P., O'Connell, P.E., 2008. RainSim: a spatial-temporal stochastic rainfall modelling system. *Environmental Modelling and Software* 23 (12), 1356–1369.
- CBS, 2008. Statline Electronic Database (www.statline.nl). Statistics Netherlands (CBS), The Hague, the Netherlands.
- Challinor, A.J., Ewert, F., Arnold, S., Simelton, E., Fraser, E., 2009. Crops and climate change: progress, trends, and challenges in simulating impacts and informing adaptation. *Journal of Experimental Botany* 10 (10), 2775–2789.
- Christensen, J.H., Carter, T.R., Rummukainen, M., Amanatidis, G., 2007. Evaluating the performance and utility of regional climate models: the PRUDENCE project. *Climatic Change* 81 (Supplement 1), 1–6.
- Christensen, J.H., Boberg, F., Christensen, O.B., Lucas-Picher, P., 2008. On the need for bias correction of regional climate change projections of temperature and precipitation. *Geophysical Research Letters* 35 (20).
- Collins, M., 2007. Ensembles and probabilities: a new era in the prediction of climate change. *Philosophical Transactions of the Royal Society A: Mathematical, Physical and Engineering Sciences* 365 (1857), 1957–1970.
- Dankers, R., Feyen, L., 2009. Flood hazard in Europe in an ensemble of regional climate scenarios. *Journal of Geophysical Research* 114 (D16), D16108.
- Darracq, A., Greffe, F., Hannerz, F., Destouni, G., Cvetkovic, V., 2005. Nutrient transport scenarios in a changing Stockholm and Mälaren valley region. *Water Science and Technology* 51 (3–4), 31–38.
- De Jonge, M., Van de Vijver, B., Blust, R., Bervoets, L., 2008. Responses of aquatic organisms to metal pollution in a lowland river in Flanders: a comparison of diatoms and macroinvertebrates. *The Science of the Total Environment* 407 (1), 615–629.
- De Weert, J., Streminska, M., Hua, D., Grotenhuis, T., Langenhoff, A., Rijnaarts, H., 2010. Nonylphenol mass transfer from field-aged sediments and subsequent biodegradation in reactors mimicking different river conditions. *Journal of Soils and Sediments* 10 (1), 77–88.
- De Wit, M., van den Hurk, B., Warmerdam, P., Torfs, P., Roulin, E., van Deursen, W., 2007. Impact of climate change on low-flows in the river Meuse. *Climatic Change* 82 (3), 351–372.
- Destouni, G., Darracq, A., 2009a. Nutrient cycling and N₂O emissions in a changing climate: the subsurface water system role. *Environmental Research Letters* 4 (3).
- Destouni, G., Darracq, A., 2009b. Nutrient cycling and N₂O emissions in a changing climate: the subsurface water system role. *Environmental Research Letters* 4 (035008).
- Destouni, G., Asokan, S.M., Jarsjö, J., 2010. Inland hydro-climatic interaction: effects of human water use on regional climate. *Geophysical Research Letters* 37 (18), L18402.
- Ek, M.B., Holtzlag, A.A.M., 2004. Influence of soil moisture on boundary layer cloud development. *Journal of Hydrometeorology* 5 (1), 86–99.
- EU, 2008. Directive 2008/105/EC of the European Parliament and of the Council on Environmental Quality Standards in the Field of Water Policy.
- EU, 2009. Common Implementation Strategy for the Water Framework Directive (2000/60/EC) Guidance document No. 24: River Basin Management in a Changing Climate (Technical Report — 2009-040).
- FAO, 1986. *Irrigation Water Management: Irrigation Water Needs*. FAO, Rome.
- Ferguson, I.M., Maxwell, R.M., 2011. Hydrologic and land-energy feedbacks of agricultural water management practices. *Environmental Research Letters* 6 (1), 014006.
- Feyen, L., Dankers, R., 2009. Impact of global warming on streamflow drought in Europe. *Journal of Geophysical Research* 114 (D17), D17116.
- Ficklin, D.L., Luo, Y., Luedeling, E., Zhang, M., 2009. Climate change sensitivity assessment of a highly agricultural watershed using SWAT. *Journal of Hydrology* 374 (1–2), 16–29.
- Ficklin, D.L., Luedeling, E., Zhang, M., 2010. Sensitivity of groundwater recharge under irrigated agriculture to changes in climate, CO₂ concentrations and canopy structure. *Agricultural Water Management* 97 (7), 1039–1050.
- Fowler, H.J., Kilsby, C.G., 2007. Using regional climate model data to simulate historical and future river flows in northwest England. *Climatic Change* 80 (3–4), 337–367.
- Fowler, H.J., Blenkinsop, S., Tebaldi, C., 2007. Linking climate change modelling to impacts studies: recent advances in downscaling techniques for hydrological modelling. *International Journal of Climatology* 27 (12), 1547–1578.

- Futter, M.N., Helliwell, R.C., Hutchins, M., Aherne, J., 2009. Modelling the effects of changing climate and nitrogen deposition on nitrate dynamics in a Scottish Mountain catchment. *Hydrology Research* 40 (2–3), 153–166.
- Gerzabek, M.H., Barcelo, D., Bellin, A., Rijnaarts, H.H.M., Slob, A., Darmendrail, D., Fowler, H.J., Négrel, P., Frank, E., Grathwohl, P., Kuntz, D., Barth, J.A.C., 2007. The integrated project AquaTerra of the EU sixth framework lays foundations for better understanding of river-sediment-soil-groundwater systems. *Journal of Environmental Management* 84 (2), 237–243.
- Goderniaux, P., Brouyère, S., Fowler, H.J., Blenkinsop, S., Therrien, R., Orban, P., Dassargues, A., 2009. Large scale surface-subsurface hydrological model to assess climate change impacts on groundwater reserves. *Journal of Hydrology* 373 (1–2), 122–138.
- Gordon, C., Cooper, C., Senior, C.A., Banks, H., Gregory, J.M., Johns, T.C., Mitchell, J.F.B., Wood, R.A., 2000. The simulation of SST, sea ice extents and ocean heat transports in a version of the Hadley Centre coupled model without flux adjustments. *Climate Dynamics* 16 (2), 147–168.
- Graham, L., Andréasson, J., Carlsson, B., 2007. Assessing climate change impacts on hydrology from an ensemble of regional climate models, model scales and linking methods – a case study on the Lule River basin. *Climatic Change* 81, 293–307.
- Groenendijk, P., Van den Eertwegh, G.A.P.H., 2004. Drainage-water travel times as a key factor for surface water contamination. In: Feddes, R.A., De Rooij, G.H., Van Dam, J.C. (Eds.), *Unsaturated Zone Modeling. Progress, Challenges and Applications*. Wageningen UR Frontis Series, vol. 6. Kluwer Ac. Pub. Dordrecht, pp. 145–178. the Netherlands. Kluwer Ac. Pub., Dordrecht, the Netherlands.
- Gül, G.O., Rosbjerg, D., Gül, A., Ondracek, M., Dikgola, K., 2010. Assessing climate change impacts on river flows and environmental flow requirements at catchment scale. *Ecology* 3 (1), 28–40.
- Hagemann, S., Jacob, D., 2007. Gradient in the climate change signal of European discharge predicted by a multi-model ensemble. *Climatic Change* 81, 309–327.
- Heijboer, D., Nellestijn, J., 2002. *Climate Atlas of The Netherlands, Normal Period 1971–2000* (in Dutch). KNMI, De Bilt, The Netherlands.
- Jacob, D., Barring, L., Christensen, O.B., Christensen, J.H., De Castro, M., Déqué, M., Giorgi, F., Hagemann, S., Hirschi, M., Jones, R., Kjellström, E., Lenderink, G., Rockel, B., Sánchez, E., Schär, C., Seneviratne, S.I., Somot, S., Van Ulden, A., Van Den Hurk, B., 2007. An inter-comparison of regional climate models for Europe: model performance in present-day climate. *Climatic Change* 81 (Supplement 1), 31–52.
- Jacoby, H.D., 1990. *Water quality*. In: Waggoner, P.E. (Ed.), *Climate Change and U.S. Water Resources*. John Wiley and Sons, New York, pp. 307–328.
- Jennings, E., Allott, N., Pierson, D.C., Schneiderman, E.M., Lenihan, D., Samuelsson, P., Taylor, D., 2009. Impacts of climate change on phosphorus loading from a grassland catchment: implications for future management. *Water Research* 43 (17), 4316–4326.
- Kay, A.L., Davies, H.N., 2008. Calculating potential evaporation from climate model data: a source of uncertainty for hydrological climate change impacts. *Journal of Hydrology* 358 (3–4), 221–239.
- Kilsby, C.G., Jones, P.D., Burton, A., Ford, A.C., Fowler, H.J., Harpham, C., James, P., Smith, A., Wilby, R.L., 2007. A daily weather generator for use in climate change studies. *Environmental Modelling and Software* 22 (12), 1705–1719.
- Koster, R.D., Dirmeyer, P.A., Guo, Z., Bonan, G., Chan, E., Cox, P., Gordon, C.T., Kanae, S., Kowalczyk, E., Lawrence, D., Liu, P., Lu, C.-H., Malyshev, S., McAvaney, B., Mitchell, K., Mocko, D., Oki, T., Oleson, K., Pitman, A., Sud, Y.C., Taylor, C.M., Verseghy, D., Vasic, R., Xue, Y., Yamada, T., 2004. Regions of strong coupling between soil moisture and precipitation. *Science* 305 (5687), 1138–1140.
- Kroes, J.G., Bonten, L.T.C., Groenendijk, P., Van der Grift, B., 2008a. Dynamic modeling of cadmium and zinc transport in the Keersop catchment (in Dutch). *Alterra Report* 1643. Wageningen, the Netherlands.
- Kroes, J.G., Van Dam, J.C., Groenendijk, P., Hendriks, R.F.A., Jacobs, C.M.J., 2008b. *SWAP version 3.2. Theory description and user manual*. Alterra-Report 16491566-7197Alterra, Wageningen, the Netherlands.
- Kroes, J.G., Bonten, L.T.C., Van der Grift, B., 2009. Long term high resolution heavy metal leaching from soils to surface waters in a Dutch catchment. *Geophysical Research Abstracts* 11 EGU2009-8130-1.
- Kroon, T., Finke, P.A., Peereboom, I., Beusen, A.H.W., 2001. Redesign STONE. The new schematization of STONE: the spatial classification and assignment of hydrological and chemical soil parameters. *RIZA-report* 2001.017. RIZA, Lelystad. 9036953713 (in Dutch).
- Kyselý, J., Beranová, R., 2009. Climate-change effects on extreme precipitation in central Europe: uncertainties of scenarios based on regional climate models. *Theoretical and Applied Climatology* 95 (3), 361–374.
- Lobell, D., Bala, G., Mirin, A., Phillips, T., Maxwell, R., Rotman, D., 2009. Regional differences in the influence of irrigation on climate. *Journal of Climate* 22 (8), 2248–2255.
- Makaske, G.B., Vissenberg, H.A., Van Grinsven, J.J.M., Tiktak, A., Sauter, F.J., 1995. *Metras: a one-dimensional model for assessment of leaching of trace metals from soil*. RIVM-report 715501005. RIVM, Bilthoven, the Netherlands. (in Dutch).
- Mavromatis, T., 2009. Use of drought indices in climate change impact assessment studies: an application to Greece. *International Journal of Climatology* 30 (9), 1336–1348.
- Milly, P.C.D., Betancourt, J., Falkenmark, M., Hirsch, R.M., Kundzewicz, Z.W., Lettenmaier, D.P., Stouffer, R.J., 2008. CLIMATE CHANGE: stationarity is dead: whither water management? *Science* 319 (5863), 573–574.
- Mínguez, M., Ruiz-Ramos, M., Díaz-Ambrona, C., Quemada, M., Sau, F., 2007. First-order impacts on winter and summer crops assessed with various high-resolution climate models in the Iberian Peninsula. *Climatic Change* 81, 343–355.
- Mulholland, P.J., Best, G.R., Coutant, C.C., Hornberger, G.M., Meyer, J.L., Robinson, P.J., Stenberg, J.R., Turner, R.E., Vera-Herrera, F., Wetzel, R.G., 1997. Effects of climate change on freshwater ecosystems of the south-eastern United States and the Gulf Coast of Mexico. *Hydrological Processes* 11 (8), 949–970.
- Nakicenovic, N., Alcamo, J., Davis, G., De Vries, H.J.M., Fenhann, J., Gaffin, S., Gregory, K., Grubler, A., Jung, T.Y., Kram, T., La Rovere, E.L., Michaelis, L., Mori, S., Morita, T., Papper, W., Pitcher, H., Price, L., Riahi, K., Roehrl, A., Rogner, H.-H., Sankovski, A., Schlesinger, M., Shukla, P., Smith, S., Swart, R., Van Rooijen, S., Victor, N., Dadi, Z., 2000. *Emissions scenarios. A Special Report of Working Group III of the Intergovernmental Panel on Climate Change*. Cambridge University Press, Cambridge.
- Nash, J.E., Sutcliffe, J.V., 1970. River flow forecasting through conceptual models part I – a discussion of principles. *Journal of Hydrology* 10 (3), 282–290.
- Oki, T., Agata, Y., Kanae, S., Saruhashi, T., Musiaka, K., 2003. Global water resources assessment under climatic change in 2050 using TRIP. *IAHS-AISH Publication*(280), pp. 124–133.
- Olesen, J., Carter, T., Díaz-Ambrona, C., Fronzek, S., Heidmann, T., Hickler, T., Holt, T., Mínguez, M., Morales, P., Palutikof, J., Quemada, M., Ruiz-Ramos, M., Rubæk, G., Sau, F., Smith, B., Sykes, M., 2007. Uncertainties in projected impacts of climate change on European agriculture and terrestrial ecosystems based on scenarios from regional climate models. *Climatic Change* 81, 123–143.
- Onușelul Gül, G., Rosbjerg, D., 2010. Modelling of hydrologic processes and potential response to climate change through the use of a multisite SWAT. *Water and Environment Journal* 24 (1), 21–31.
- Park, M.J., Park, J.Y., Shin, H.J., Lee, M.S., Park, G.A., Jung, I.K., Kim, S.J., 2010. Projection of future climate change impacts on nonpoint source pollution loads for a forest dominant dam watershed by reflecting future vegetation canopy in a soil and water assessment tool model. *Water Science and Technology* 61 (8), 1975–1986.
- Pieterse, N.M., Bleuten, W., Jørgensen, S.E., 2003. Contribution of point sources and diffuse sources to nitrogen and phosphorus loads in lowland river tributaries. *Journal of Hydrology* 271 (1–4), 213–225.
- Pope, V.D., Gallani, M.L., Rowntree, P.R., Stratton, R.A., 2000. The impact of new physical parametrizations in the Hadley Centre climate model: HadAM3. *Climate Dynamics* 16 (2), 123–146.
- Prudhomme, C., Reynard, N., Crooks, S., 2002. Downscaling of global climate models for flood frequency analysis: where are we now? *Hydrological Processes* 16 (6), 1137–1150.
- Roeckner, E., Arpe, K., Bengtsson, L., Christoph, M., Clausen, M., Dümenil, L., Esch, M., Giorgetta, M., Schlese, U., Schulzweida, U., 1996. The atmospheric general circulation model ECHAM-4: model description and simulation of present-day climate. Report no 218. Max-Planck Institute for Meteorology, Hamburg, Germany.
- Rozemeijer, J., 2002. Heavy metals in the unsaturated zone. TNO-report NITG 02-081-A. TNO-NITG, Utrecht, the Netherlands. (in Dutch).
- Rozemeijer, J.C., Broers, H.P., 2007. The groundwater contribution to surface water contamination in a region with intensive agricultural land use (Noord-Brabant, The Netherlands). *Environmental Pollution* 148 (3), 695.
- Rozemeijer, J.C., Van der Velde, Y., Van Geer, F.C., Bierkens, M.F.P., Broers, H.P., 2010. Direct measurements of the tile drain and groundwater flow route contributions to surface water contamination: from field-scale concentration patterns in groundwater to catchment-scale surface water quality. *Environmental Pollution* 158 (12), 3571–3579.
- Schiedek, D., Sundelin, B., Readman, J.W., Macdonald, R.W., 2007. Interactions between climate change and contaminants. *Marine Pollution Bulletin* 54 (12), 1845–1856.
- Scibek, J., Allen, D.M., 2006. Modeled impacts of predicted climate change on recharge and groundwater levels. *Water Resources Research* 42 (11), W11405.
- Shibuo, Y., Jarsjö, J., Destouni, G., 2007. Hydrological responses to climate change and irrigation in the Aral Sea drainage basin. *Geophysical Research Letters* 34 (21), L21406.
- Sjøeng, A.M.S., Kaste, Ø., Wright, R.F., 2009. Modelling future NO₃ leaching from an upland headwater catchment in SW Norway using the MAGIC

- model: II. Simulation of future nitrate leaching given scenarios of climate change and nitrogen deposition. *Hydrology Research* 40 (2–3), 217–233.
- Tebaldi, C., Knutti, R., 2007. The use of the multi-model ensemble in probabilistic climate projections. *Philosophical Transactions of the Royal Society A: Mathematical, Physical and Engineering Sciences* 365 (1857), 2053–2075.
- Thodsen, H., Hasholt, B., Kjærsgaard, J.H., 2008. The influence of climate change on suspended sediment transport in Danish rivers. *Hydrological Processes* 22 (6), 764–774.
- Van Bakel, P.J.T., Massop, H.T.L., Kroes, J.G., Hoogewoud, J., Pastoors, M.J.H., Kroon, T., 2008. Updating the hydrology component in STONE 2.3: adjustment boundary conditions and parameters, linking NAGROM and SWAP, plausibility test. Statutory Research Tasks Unit for Nature and the Environment. WOt-report 57. Wageningen, the Netherlands.
- Van der Grift, B., Griffioen, J., 2008. Modelling assessment of regional groundwater contamination due to historic smelter emissions of heavy metals. *Journal of Contaminant Hydrology* 96 (1–4), 48–68.
- Van der Velde, Y., De Rooij, G.H., Rozemeijer, J.C., Van Geer, F.C., Broers, H.P., 2010. Nitrate response of a lowland catchment: on the relation between stream concentration and travel time distribution dynamics. *Water Resources Research* 46 (11), W11534.
- Van Pelt, S.C., Kabat, P., Ter Maat, H.W., Van Den Hurk, B.J.J.M., Weerts, A.H., 2009. Discharge simulations performed with a hydrological model using bias corrected regional climate model input. *Hydrology and Earth System Sciences* 13 (12), 2387–2397.
- Van Roosmalen, L., Christensen, B.S.B., Sonnenborg, T.O., 2007. Regional differences in climate change impacts on groundwater and stream discharge in Denmark. *Vadose Zone Journal* 6 (3), 554.
- Van Roosmalen, L., Christensen, J.H., Butts, M.B., Jensen, K.H., Refsgaard, J.C., 2010. An intercomparison of regional climate model data for hydrological impact studies in Denmark. *Journal of Hydrology* 380 (3–4), 406–419.
- Van Vliet, M.T.H., Zwolsman, J.J.G., 2008. Impact of summer droughts on the water quality of the Meuse river. *Journal of Hydrology* 353 (1–2), 1–17.
- Van Vliet, M.T.H., Blenkinsop, S., Burton, A., Harpham, C., Broers, H.P. and Fowler, H.J., in press. A multi-model ensemble of downscaled spatial climate change scenarios for the Dommel catchment, Western Europe. *Climatic Change*. doi:10.1007/s10584-011-0131-8.
- Visser, A., Broers, H.P., Van der Grift, B., Bierkens, M.F.P., 2007. Demonstrating trend reversal of groundwater quality in relation to time of recharge determined by $^3\text{H}/^3\text{He}$. *Environmental Pollution* 148 (3), 797–807.
- Visser, A., Broers, H.P., Heerink, R., Bierkens, M.F.P., 2009. Trends in pollutant concentrations in relation to time of recharge and reactive transport at the groundwater body scale. *Journal of Hydrology* (3–4), 427–439.
- Vogel, J.C., 1967. Investigation of groundwater flow with radiocarbon. IAEA Symposium on Isotopes in Hydrology, 14–18 November 1966. IAEA, Vienna, Austria, pp. 355–369.
- Vörösmarty, C.J., Green, P., Salisbury, J., Lammers, R.B., 2000. Global Water Resources: vulnerability from climate change and population growth. *Science* 289 (5477), 284–288.
- Wang, G.L., Kim, Y.J., Wang, D.G., 2007. Quantifying the strength of soil moisture-precipitation coupling and its sensitivity to changes in surface water budget. *Journal of Hydrometeorology* 8, 551–570.
- Watts, M., Goodess, C.M., Jones, P.D., 2004. The CRU daily weather generator. BETWIXT Technical Briefing Note 1, Version 2. February.
- Weber, F.A., Hofacker, A.F., Voegelin, A., Kretzschmar, R., 2010. Temperature dependence and coupling of iron and arsenic reduction and release during flooding of a contaminated soil. *Environmental Science & Technology* 44 (1), 116–122.
- Wegehenkel, M., 2009. Modeling of vegetation dynamics in hydrological models for the assessment of the effects of climate change on evapotranspiration and groundwater recharge. *Advances in Geosciences* 21, 109–115.
- Wegehenkel, M., Kersebaum, K.C., 2009. An assessment of the impact of climate change on evapotranspiration, groundwater recharge, and low-flow conditions in a mesoscale catchment in Northeast Germany. *Journal of Plant Nutrition and Soil Science* 172 (6), 737–744.
- Whitehead, P.G., Wade, A.J., Butterfield, D., 2009. Potential impacts of climate change on water quality and ecology in six UK rivers. *Hydrology Research* 40 (2–3), 113–122.
- Wilby, R.L., Wigley, T.M.L., 1997. Downscaling general circulation model output: a review of methods and limitations. *Progress in Physical Geography* 21 (4), 530–548.
- Wilby, R.L., Whitehead, P.G., Wade, A.J., Butterfield, D., Davis, R.J., Watts, G., 2006. Integrated modelling of climate change impacts on water resources and quality in a lowland catchment: River Kennet, UK. *Journal of Hydrology* 330 (1–2), 204–220.
- Wösten, J.H.M., 1994. Water retention and permeability characteristics of top and subsoils in the Netherlands: the Staring series. DLO-Staring Centrum, Wageningen, the Netherlands. New edition. (in Dutch).
- Yu, P.S., Wang, Y.C., 2009. Impact of climate change on hydrological processes over a basin scale in northern Taiwan. *Hydrological Processes* 23 (25), 3556–3568.